LAKE CHAD: RECENT DRY SEASON AREA CHANGES, NEAR TERM DRY SEASON AREA PROJECTIONS, AND DRY SEASON AREA PROJECTIONS THROUGH THE YEAR 2100

by
Frederick S. Policelli

A dissertation submitted to Johns Hopkins University in conformity with the requirements for the degree of Doctor of Philosophy

Baltimore, Maryland
December, 2018

Lake Chad, in the Sahel region of Africa is shallow, freshwater, and the terminal lake of an enormous (2.5 million km^2) endorheic basin. The lake has exhibited a wide range of area over the centuries. More recently, some of the earliest satellite photographs of Lake Chad were taken in the 1960s when the lake area was estimated to be about 25,000 km^2. During the late 1960s, the 1970s and the 1980s, a recurrent set of droughts caused the lake area to decrease sharply. During the period when the lake was drying, large areas of aquatic vegetation formed in the lake, while a small area of open water persisted. It appears likely that some researchers and the popular press have focused only on the small open water area when reporting the size of Lake Chad, because it is very challenging to detect and measure the area of flooded vegetation. Reports of a decrease of ninety to ninety-five percent of lake area, relative to lake area in the 1960s, led the Lake Chad Basin Commission (LCBC) to study an interbasin water transfer from the Ubangi River, a tributary to the Congo River.

The motivation for this dissertation was to use satellite data and modeling results to provide information on the recent trends of total Lake Chad area (open water and flooded vegetation), and to provide statistical models and results for near term and long term modeling of the lake area. This dissertation provides indications that, while highly variable, the area of Lake Chad has been increasing in recent years and the area of the lake can be forecast with reasonable accuracy for the next dry season months. Additionally, under the "baseline" climate scenario (Representative Concentration Pathway 8.5) modeled by the Coupled Model Intercomparison Project 5 and our statistical model of lake area, the lake is projected to persist during dry seasons through the twenty-first century, and is even likely to grow larger during that time.

Readers: Ben Zaitchik, Kevin Lewis

Advisor: Ben Zaitchik

Acknowledgments

The following people had significant influence on this dissertation and are my co-authors on journal papers resulting from this dissertation: Ben Zaitchik, Alfred Hubbard, Hahn Chul Jung, and Charles Ichoku.

Considerable funding support for this dissertation was provided by the NASA Goddard Space Flight Center's Academic Investment for Mission Success (AIMS) Program.

I would also like to thank my wife, Carol Policelli, for her continuous love, patience, and support during the writing of this dissertation.

Publications and Co-authors

The first chapter of this dissertation was published in Remote Sensing (Policelli et al., 2018a, co-authors: Alfred Hubbard, Hahn Chul Jung, Ben Zaitchik, Charles Ichoku). The second chapter of this dissertation was published in Journal of Hydrology (Policelli et al., 2018b, co-authors: Alfred Hubbard, Hahn Chul Jung, Ben Zaitchik, Charles Ichoku). The third chapter of this dissertation is being prepared for submission to Climatic Change (co-authors: Ben Zaitchik, Alfred Hubbard, Hahn Chul Jung, Charles Ichoku).

Table of Contents

List of Tables

List of Figures

List of Figures

Introduction

Lake Chad, in the Sahel region of Africa is shallow, freshwater, and the terminal lake of an enormous (2.5 million km^2) endorheic basin. In 2014, over two million people lived along the shoreline of Lake Chad (Magrin, 2016), and by 2015, the lake provided a livelihood for an estimated thirteen million people (Bouchez et al., 2016). The lake has exhibited a wide range of area over the centuries. Using a Digital Elevation Model derived from data from the NASA Shuttle Radar Topography Mission and Landsat satellite data, (Schuster et al., 2005) found that the Holocene "Lake Mega Chad" had an area greater than 350,000 km^2 (Fig. I.1). Today it would be the second largest freshwater lake in the world. In our own time, some of the earliest space-based photographs of Lake Chad were taken by the NASA Gemini (1965) and Apollo (1968) astronauts. At that time, the lake area was estimated to be about 25,000 km^2 (Birkett, 2000). During the late 1960s, the 1970s and the 1980s, a recurrent set of droughts caused the lake area to decrease sharply (Birkett, 2000). Note that the annual flooding of Lake Chad takes place during the dry season

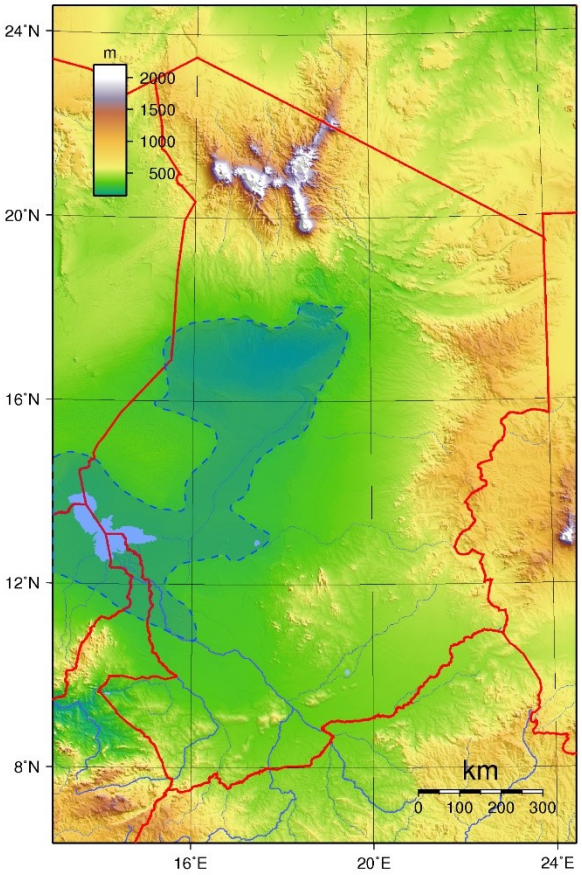

Fig. I.1 Modern Lake Chad (light blue, Lake Mega Chad (outlined with blue dashes). Chad is outlined in red (center) commons.wikimedia.org

(November through May). Data from Leblanc et al. [2011] provide an estimated average of the 1988-1989 dry season through the 1992-1993 dry season average lake area at about 9,800 km^2. From the data for Policelli et al. [2018a], we found the average of the 2012-2013 dry season through the 2016-2017 dry season average lake area to be approximately 14,500 km^2.

During the period when the lake was drying, large areas of aquatic vegetation formed in the lake (Leblanc et al., 2011), while a small area of open water persisted. It appears likely that some researchers (e.g. Gao et al., 2011), and the popular press have focused only on the small open water area when reporting the size of Lake Chad, because it is very challenging to detect and measure the area of flooded vegetation. Reports of a decrease of ninety to ninety-five percent of lake area, relative to lake area in the 1960s, led the Lake Chad Basin Commission (LCBC) to study an interbasin water transfer from the Ubangi River, which forms the border between the Democratic Republic of the Congo and the Central African Republic, and is a tributary to the Congo River. A Canadian firm, CIMA International, was contracted to lead a feasibility study on the water transfer concept during 2009-2011. The study concluded that the project was technically feasible and estimated the cost at $14.5 billion. In 2012, the study results were endorsed by the heads of state of the member nations of the LCBC (https://www.environewsnigeria.com/inter-basin-water-transfer-opportunities-prospects-lake-chad/, 2018).

The motivation for the dissertation was to use satellite data and modeling results to provide information on the recent trends of total Lake Chad area (open water and flooded vegetation), and to provide statistical models and results for near term and long term modeling of the lake area. We hope that the outcome will be to (1) help inform the on-going discussion about the area of Lake Chad and plans to transfer water to the lake from the Congo Basin, and (2) to provide methods that the Lake Chad Basin Commission (or others) could use to inform stakeholders on the area and projected area of the lake.

This dissertation consists of an introduction, three manuscripts for journal articles developed in collaboration with four co-authors, and a conclusion. At the time of writing, the first and second articles have been published, and the third is being prepared for submission. In the first article, entitled, "Lake Chad total surface water area as derived from Land Surface Temperature and radar remote sensing data" we use LST data from the MODerate resolution Imaging Spectroradiometer (MODIS) sensor on the NASA Terra satellite to identify and measure areas of open water and flooded vegetation during the dry season and within the boundaries of the lake. We use ESA Sentinel-1a C-band radar data to bias correct the area of the lake and we extend the record of the lake area using bias corrected lake areas derived from LST data from the EUMETSAT Meteosat Visible and InfraRed Imager (MVIRI) sensor by (Leblanc et al., 2011). LST and radar data are used because they can provide information about both open water and water under vegetation canopy. The result is a time series of Lake Chad area for the 1988-1989 dry season through the 2016-2017 dry season. The time series appears to be periodic in nature, with a trend line increasing at a moderate rate.

The second paper, "A predictive model for Lake Chad total surface water area using remotely sensed and modeled hydrological and meteorological parameters and multivariate regression analysis" focuses on developing a statistical model of the area of Lake Chad using satellite-based observations and model data of the southern part of the basin and lake parameters related to lake area. The southern part of the basin includes essentially all of the area from which runoff reaches the lake, plus the lake itself. We use linear first order regression and backward elimination to optimize equations for lake area with three independent variables for each of the dry season months. The set of independent variables from which we select are: wet season southern basin precipitation, wet season southern basin evapotranspiration, lake evapotranspiration as a percentage of the 1988-2016 average,

November lake elevation variation relative to the 2002-2009 average, and the previous year's lake area for the given month. We limit the equations to three independent variables to avoid overfitting. The resulting equations can be used in late November to estimate the December average monthly total lake area, and in early December to make estimates for January to May. Using a Leave One Out Cross Validation (LOOCV) analysis, we estimate the average error for the statistical model to range from 5.3 percent to 7.6 percent.

In the third paper, "Projections of Lake Chad total surface water area derived by forcing a statistical model of the lake area with results of climate simulations through the year 2100" we again develop statistical models for each month of the dry season, though this time only using wet season precipitation, wet season evapotranspiration, and the previous year's area for the given month. Then, using the model training data, we bias correct the precipitation and evapotranspiration data for 1993-2100 from seventy-four Global Climate Model simulations performed for the Coupled Model Intercomparison Project 5 (CMIP5, Taylor et al., 2011) and run under the Representative Concentration Pathway 8.5 (RCP 8.5) scenario. We then use the bias corrected simulation data in our statistical model and average the monthly data to dry season average. Note that the statistical model is initialized for the first year with observation-based lake area from the research for our first paper, and then it keeps track of the previous year's area internal to the model. Next we average the results from the eleven models provided as ensemble members to generate an additional eleven simulations. The result is eighty-five time series of projected average dry season lake area for 2000-2100. Not one of the eighty-five time series of average dry season lake area drops below about 4,500 km^2. The slope of the trend line of the average of the time series is positive; in other words, for the set of available simulations, and as calculated by our statistical model, on average the dry season average area of the lake is projected to increase. We additionally use several criteria to downselect climate models that should perform the best. First we use

model performance during the period of observations as the criteria for selecting models. This results in a selection of six CMIP5 RCP 8.5 models (21 simulations including all of the ensemble members). The slope of the trend line of projected area derived from the average of the simulations is significantly higher than for the trend line derived from the average of the original set of eighty-five simulations. For these simulations, the average dry season lake area does not drop below 9,900 km^2. Next we use climate models that perform well modeling precipitation in central Africa (including the Lake Chad catchment) per Fotso-Nguemo Thierry C. et al. [2018] as our criteria for selecting models expected to perform well. This results in a selection of nine CMIP5 RPC 8.5 models (23 simulations including all of the ensemble members). Again the slope of the trend line of projected area derived from the average of the simulations is significantly higher than for the trend line derived from the average of the original set of eighty-five simulations. For this set of simulations, the derived area does not drop below 8,100 km^2.

Taken as a whole, this dissertation provides indications that, while highly variable, the area of Lake Chad has been increasing in recent years, the area of the lake can be forecast with reasonable accuracy for the next dry season months, the lake is projected to persist through the dry seasons of the twenty-first century, and it is even likely to grow larger during that time.

CHAPTER 1

Lake Chad total surface water area

as derived from land surface temperature

and radar remote sensing data

1.1 Introduction

Lake Chad and Environment

Lake Chad is a large endorheic lake located in central Africa and intersecting the Sudan-Savanna, Sahelian, and Saharan agro-climatic zones (Sarch and Birkett, 2000). The Lake Chad Basin (Figure 1.1), at approximately 2.5 million km^2, is the world's largest endorheic basin, though much of the basin lies in the Sahara Desert and only about one-third of the basin (the southern portion) is hydrologically active (Bouchez et al., 2016). Roughly ninety percent of the water reaching Lake Chad is provided by the Chari-Logone River (Birkett, 2000). The Chari and Logone Rivers join at N'Djamena, Chad and flow a short distance to discharge through a delta formation into Lake Chad. The Chari contributes roughly sixty percent of the flow to the Chari-Logone River, with the remaining forty percent coming from the Logone (Delclaux et al., 2008). An additional two percent of Lake Chad's water comes from the Komadougou-Yobe River (also known as the Yobe River, Gao et al., 2011), which flows through Niger and Nigeria to the west of the lake. The remaining water input comes from direct rainfall on the lake and some smaller tributaries. Water leaves the lake primarily through evapotranspiration, though an undetermined amount is believed to exit through infiltration (Lemoalle, 2004).

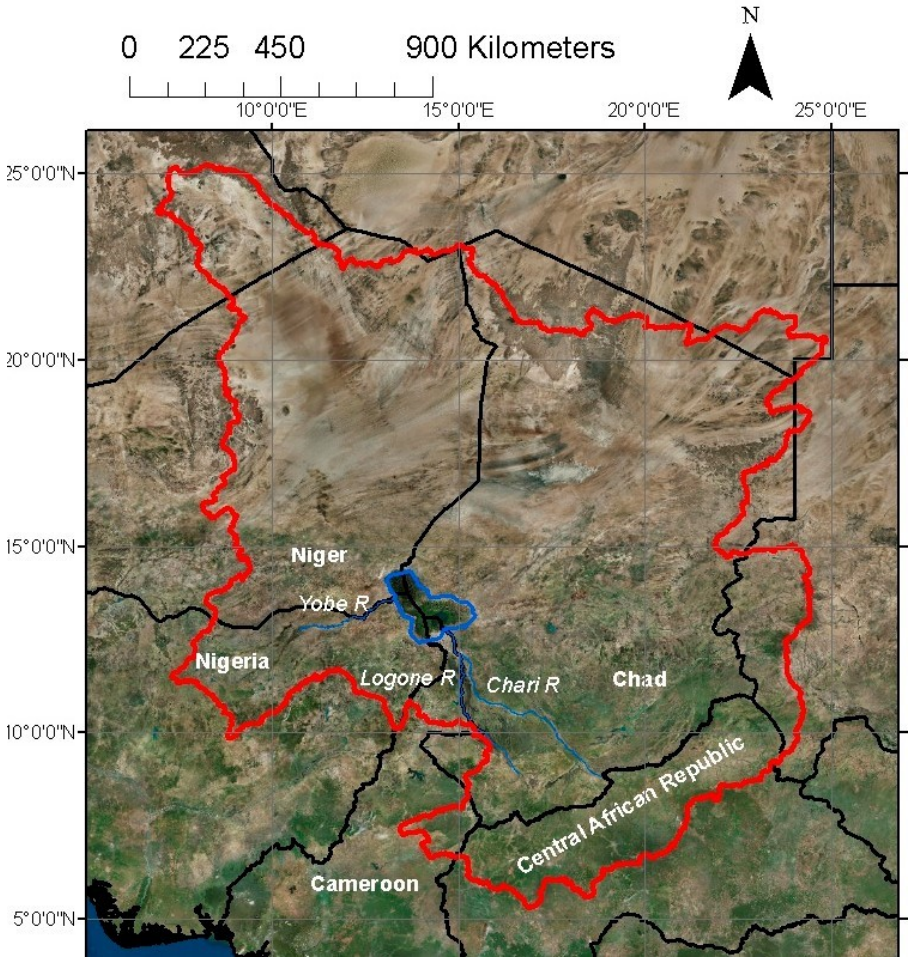

Figure 1.1 Lake Chad Basin (**red line**), Lake Chad and its main rivers (**blue lines**).

Lake Chad is shared by Chad, Niger, Nigeria, and Cameroon, while the basin additionally includes parts of the Central African Republic, Algeria, Sudan, and Libya. The surface level of the lake is roughly 282 m above sea level (Birkett, 2000), and the average depth of the lake is less than 2 m (Bader et al., 2011).

Lake Chad is well known for the dramatic decrease in surface area that occurred in the 1970s and 1980s (Grove, 1996), particularly the open (unvegetated) area of the lake, which is most readily visible from optical satellite images.

Lake Chad has marked wet and dry seasons. The wet season lasts from June to October, although due to the time lag of water flowing through the Chari and Logone River systems, the

annual flooding occurs during the dry season (Leblanc et al., 2011). The lake rises about 1–2 m during the annual flooding season (Birkett, 2000) and provides livelihoods to fishermen who are most productive following the floods, to "recession farmers" who farm in the rich soils of the receding floodwaters, and to those who raise livestock (Sarch and Birkett, 2000).

1.2 Background

Grove, 1996 states that "One of the most spectacular results of the increased aridity was the shrinkage of Lake Chad from its highest level and greatest extent this century, about 25,000 square kilometers in the 1960s to about one tenth that area in the mid 1980s." According to UNEP (a), 2006, "Lake Chad's surface area decreased from 22,902 km^2 . . . in 1963 to a mere 304 km^2 . . . in 2001." According to Gao et al., 2011, "Over the last 40 years, Lake Chad . . . has decreased by more than 90% in area." Lemoalle et al.,2012 cite a changing lake area between 1973 and 2011 "ranging between 1,800 and 15,000 km^2." These statements (Table 1.1) are not necessarily inconsistent; however it is difficult to get a clear picture of the recent total surface water area trends and variability from these sources.

Table 1.1 Descriptions of Lake Chad area changes
for extended periods found in the literature

Source	Approx Dates	L. Chad Area Change (km^2)	L. Chad Area Change (%)
Grove, 1996 [9]	1960s–mid 1980s	−22,500	−90%
UNEP, 2006 [11]	1963–2001	− 22,598	− 99%
Gao et al., 2011 [6]	1971–2011	N/A	More than −90%
Leblanc et al., 2011 [10]	1986–2001	(+) 3500 *	(+) 33% *

* difference between 1st data point (May 1986) and last data point (May 2001).

According to the World Lakes Database of the International Lake Environment Committee, Lake Chad covers 1540 km^2. Because they do not say how and when they measured that area, it is not possible to know if there was an attempt to include flooded

vegetation and whether that figure represents a minimum, a maximum or an intermediate level for the year.

The only sources found providing significant observation-based time series of area for Lake Chad are Birkett, 2000 and Leblanc et al., 2011. Their results differ significantly. Leblanc et al., 2011 used 5 km resolution Land Surface Temperature (LST) data from the Meteosat satellites operated by the European Organization for the Exploitation of Meteorological Satellites (EUMETSAT). Using this data, Leblanc et al., 2011 developed a monthly record of the lake area from 1986 to 2001, differentiating water vs. non-water using a 2-cluster unsupervised classification process. Note that this lumps dry soil, wet soil, and dry vegetation classes into a single non-water class, and water and flooded vegetation into a single water class. They avoided making the analysis during the wet season, which presumably limited misidentification of wet soil with the water classes. They suggest that the use of satellite-based radar data may be helpful for mapping both open water and water under vegetation, but cite a number of reasons for not using it, notably the limitation of available radar data at the time of their research. They conclude that during the study period, the lake minimum size was 4,600 km^2 in October 1987, the maximum size was 16,300 km^2 in February 2000, the 25th percentile area was 8,800 km^2, and the 75th percentile area was 13,700 km^2.

Birkett, 2000, on the other hand, used 1.1 km resolution Near InfraRed (NIR) data from NOAA's AVHRR on-orbit sensor to estimate the total lake surface water area from 1995 to 1999. The estimate frequency was sub-monthly. Based on the fact that water absorbs strongly in the NIR part of the spectrum, whereas healthy vegetation reflects strongly in NIR, Birkett, 2000 distinguishes marshland and open water as the darkest pixels vs. dry land as brighter pixels. As a threshold between the two, she chose the midpoint between the two characteristic peaks of the histograms for the two types of landcover, using NIR sensor digital numbers. From that analysis, she found a permanent total surface water area (open water and

marshland) of 1385 km^2 and a peak total surface water area of approximately 5000 km^2.

There are some indications from the literature that the lake has been increasing in size since the 1990s, however these patterns are either not well described or are defined over a relatively short period of time. According to UNEP (b) "the 2007 (satellite) image shows significant improvement (increased surface water area) over previous years". Several authors note a rising trend in rainfall, lake elevation, and flow to the lake starting in the 1990s. According to Biasutti and Giannini, 2006, "The African Sahel experienced severe drying between the 1950s and the 1980s, with partial recovery since." Birkett, 2000, who also notes "a possible correlation (of decreasing lake water inflows) with El Nino events", describes a rise in minimum lake levels by 15–35 cm per year and indications of increasing rainfall in parts of the basin during the period of her study (1995–1999). Lemoalle et al., 2012 note increases in mean annual Chari River stream flow recovering in the 1990s after significant drops in the 1970s and 1980s, although through the period 2000–2009, the flows were still only about half of what they were during the 1960s. Gao et al., 2011 note that, "The north lake's level continually decreased until 1986 when it dried out completely. Water reappeared in the north lake in 1999 after a few years of wet weather." Despite the evidence of changing lake size, it does not appear that the research community has created an updated time series of the lake's total surface water area since the Leblanc et al., 2011 analysis for 1986–2001.

Objectives of Study

The primary purposes of this paper are to use remote sensing data (Figure 1.2) to extend the existing total surface water area record of Lake Chad, and to provide data for calibrating a model of the annual flooding of the lake. Such a model could be very useful for supporting livelihood decisions for part of the population of the lake. Sarch and Birkett, 2000), for instance, found that "farmers cannot be sure when the flood will reach the land around their village or whether it will at all.

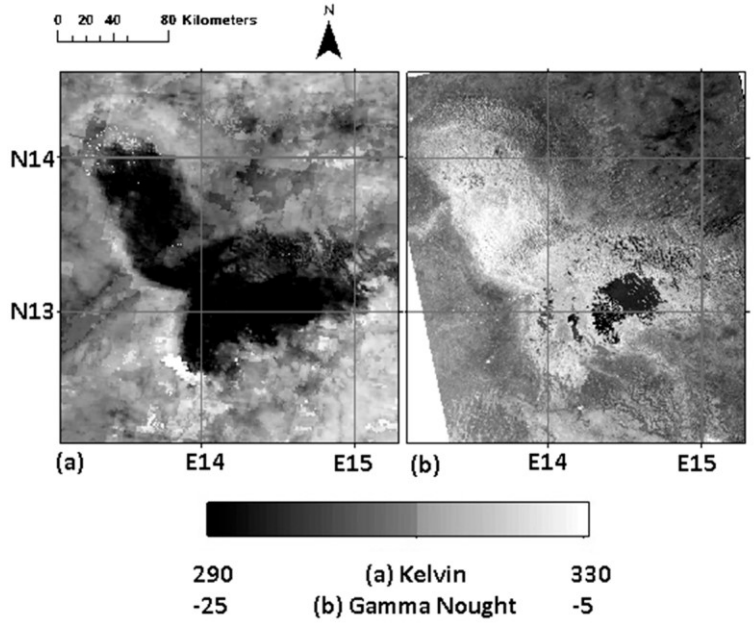

Figure 1.2. Examples of the remote sensing products used in this research (a) NASAMODIS Land Surface Temperature (LST) (9 May 2017–16 May 2017); (**b**) ESA Sentinel-1a C-band Radar (16 May 2017)

1.3 Materials and Methods

Overview of Datasets Used in this Study

The primary data sets used to determine the total surface water area of Lake Chad in this paper are the 8-day NASA MODIS Terra daytime LST product (MOD11A2, available from March 2000 to the present), the C-band radar data from ESA's Sentinel-1a mission (acquired every 12 days, available from April 2015 to May 2017), and monthly total surface water area data derived by Leblanc et al., 2011 from Meteosat maximum daily LST measurements. The data used for the research by Leblanc et al., 2011 were acquired from mid-1986 to mid-2001. Their data record for 1986 and 1987 was incomplete, so we used their area estimates from 1988 to 2001 to extend our record.

Daytime NASA MODIS LST data

The use of daytime LST data products (Wan, 2015(a), 2015(b)) for analysis of total surface water area is based on the fact that areas containing surface water (including water obscured by vegetation) generally appear cooler than areas not containing water during daytime observation because of (1) the higher thermal inertia of surface water vs. non-water pixels; (2) the potential for mixing of cooler water from below; and (3) evaporative cooling of water pixels (Leblanc et al., 2011). The use of LST was applied by Rigal, 1989 to map flooded vegetation in Lake Chad for a single dry season and by Leblanc et al., 2011 to measure the total area of Lake Chad for the period 1986–2001.

ESA Sentinel-1a C-Band Radar Imagery

Remote sensing using radar data has the advantages that it can collect data from the surface during cloud cover, and that it can penetrate vegetation canopy to a limited extent. Eighteen Sentinel-1 C-band radar data sets were identified that were acquired during the dry season and completely covered the area of interest. Note that wet season radar data appeared to be unable to distinguish between soil moisture and flooded vegetation in places and were not used in this study (Kasischke et al., 2011). The polarization configuration for these data sets was V-V. Using SAR data from the Sentinel-1a mission, we first generated multi-look amplitude images by averaging ten looks in range and ten looks in azimuth to reduce speckle noise. The ground size of a pixel resulting from this is 100 m. The amplitude images were also converted from digital number to the radar backscattering coefficient γ^0 in order to calibrate the radiometric Sentinel-1a SAR data for Lake Chad. Next, we carried out terrain correction (i.e., orthorectification) to determine the accurate locations of pixels in the multi-look images using the Shuttle Radar Topography Mission (SRTM) Digital Elevation Model (DEM). Finally, we mapped the data onto a UTM projection, and then mosaicked the images

to provide complete coverage of the lake.

Lake Area Estimation Using ESA Sentinel-1a C-Band Radar Data

We selected training sites for open water, flooded vegetation, and dry vegetation within and adjacent to the lake (see Figure 1.3). Detection of placid open water with SAR data is relatively straight forward because a transmitted radar pulse specularly reflects away from a side-looking SAR antenna giving the water very low values of backscatter (Jung and Alsdorf, 2010). The training site for open water was in the region of very dark radar pixels in the southern part of the lake and classified by the 0.5 km MODIS-based Global Land Cover Climatology (Broxton et al., 2014) as open water. The training site for dry vegetation was in the region outside of the lake boundaries and classified by the 0.5 km MODIS-based Global Land Cover Climatology (Broxton et al., 2014) as grassland. The training site for flooded vegetation was at the discharge of the Komadougou Yobe (also known as the Yobe) River. According to Lemoalle et al., 2012, "The input from the small River Yobe . . . is just sufficient to maintain a marshy area around its estuary." It was found that the dry land backscatter was greater than the open water backscatter and the flooded vegetation backscatter was greater than the dry land backscatter. The high backscatter from flooded vegetation was considered to be due to the well-known "double-bounce" effect (Jung and Alsdorf, 2010) that radar experiences in water with vertical vegetation surfaces from which to reflect.

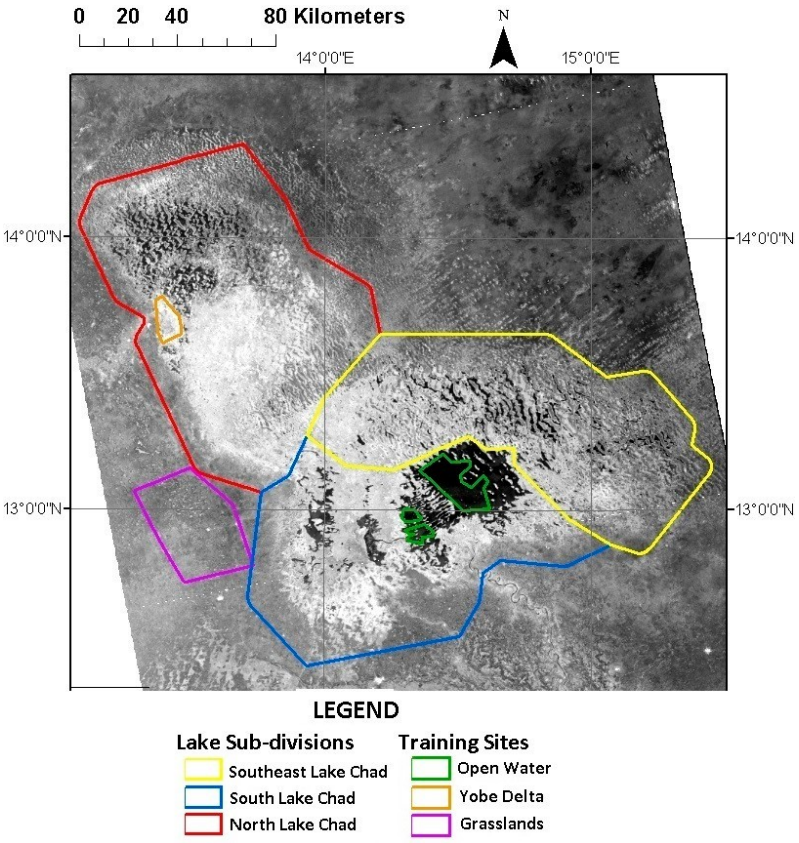

Figure 1.3. Lake sub-divisions and training sites identified in this study. The background image is from ESA Sentinel-1a C-band radar (9 April 2015).

Lake Area Estimation Using NASA MODIS Land Surface Temperature (LST) Data

As in Leblanc et al., 2011, two-class unsupervised classification was performed on the data with the assumption (for reasons described above) that open water and flooded vegetation would be represented in the cooler of the two classes. The two-class unsupervised classification was performed on the 8-day LST products, then monthly total surface water areas were estimated by interpolation from the relevant 8-day areas for comparison with Leblanc et al., 2011 and to extend the period of their monthly data record. We rejected MODIS LST datasets with higher than 5% cloud cover and/or "no data" pixels. Of the 482 8-day, dry season MODIS LST datasets, less than 4 percent were rejected for these reasons.

Comparison of Sentinel-1a Data with MODIS Land Surface Temperature (LST) Data

For the period of Sentinel-1a data (2015–early 2017), we made a comparison between the Sentinel-1a estimates of Lake Chad total surface water area and the areas of corresponding dates calculated using MODIS Land Surface Temperature data.

As a check on the spatial correlation of the SAR and LST-based maps of total surface water area, we divided the lake into three regions, (1) Southeast Lake Chad; (2) North Lake Chad; and (3) South Lake Chad, (Figure 1.3) roughly corresponding to the Archipelago, Northern Pool, and Southern Pool of the lake and made a comparison between the Sentinel-1a and MODIS LST estimates of the lake's surface water area for these sub-divisions.

Compilation of Combined Total Lake Surface Water Area Estimates

We compared the adjusted MODIS LST-derived total surface water area data to the Leblanc et al., 2011 data for the period of overlap, and made a modest bias adjustment to the Leblanc data based on the comparison.

Finally, a best estimate of the long-term time series of total lake surface water area was assembled by combining the bias adjusted findings of Leblanc et al., 2011 and the radar-adjusted, LST-based time series generated by the research for this paper.

1.4 Results

This section presents the results related to our investigation of Lake Chad total surface water area. The technique used in this study to measure the total surface water area of Lake Chad with LST measurements is severely limited by the need to use it only under dry conditions to avoid confusing soil moisture with flooded area and experiencing data loss (Figure 1.4). Note the extensive area of cool temperatures (dark areas) during the wet season and the areas of data loss (white areas) in Figure 1.4a and compare this with the dry season (Figure 1.4b).

Use of C-band radar during the wet season seems to present a similar problem by failing to distinguish between soil moisture and flooded vegetation; notice in Figure 1.5a (wet season) the boundaries of the lake are not as clear as in Figure 1.5b (dry season). However, there are applications such as measuring total surface water area in the Sudd, or the Niger inland delta, or the Okavango Delta, that would also likely benefit from using both LST and radar remote sensing approaches during their dry seasons.

In the comparison of total surface water area from Sentinel-1a C-band radar with that from MODIS LST, we found a very low difference (less than 2 percent on average).

For each of the three regions and each of the 18 pairs of data sets, we determined the total surface water area calculated using the radar data and the LST data, and the percent difference between the two. We conclude that the surface water area calculated using the LST data is considerably more (31% on average) in Southeast Lake Chad, considerably less in North Lake Chad (19% on average), and very similar in South Lake Chad (0.3% greater on average); (Table 1.2). The fact that the average area for the total lake is very close (within 2 percent) for the two different methods appears to be entirely coincidental. We found that within each subdivision of the lake, the differences between image pairs (LST and radar) appeared to be random, with no systematic pattern within or across the subdivisions as a function of time.

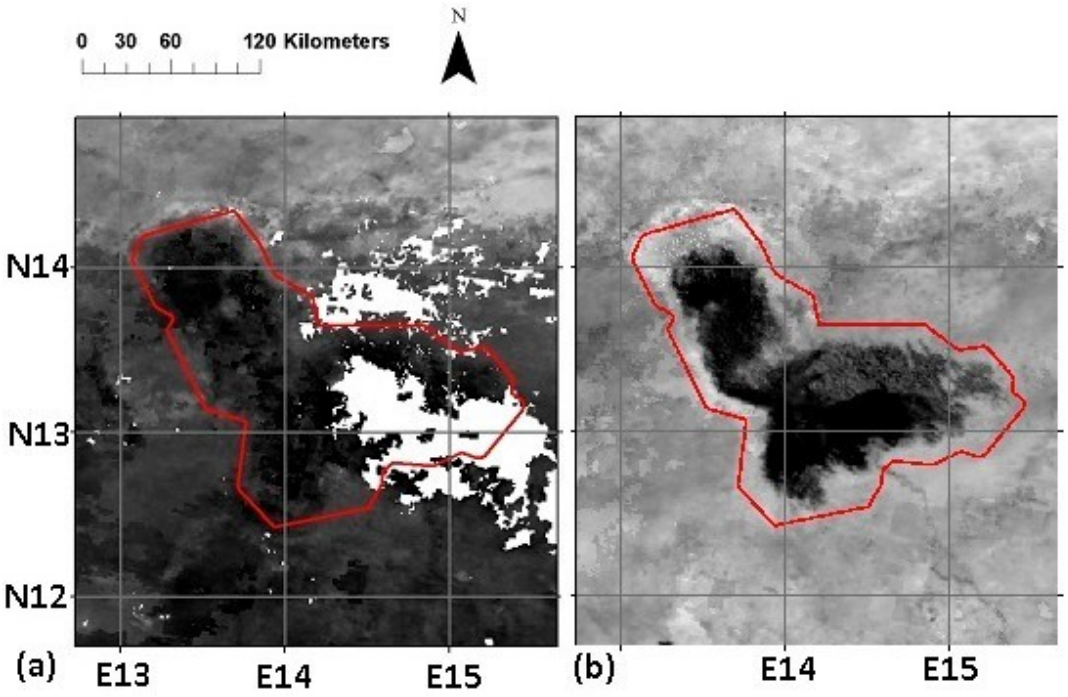

Figure 1.4. Example NASA MODIS Land Surface Temperature (LST) data during (**a**) wet season (12 August 2016) (**b**) dry season (15 April 2017) White areas in (**a**) are no data.

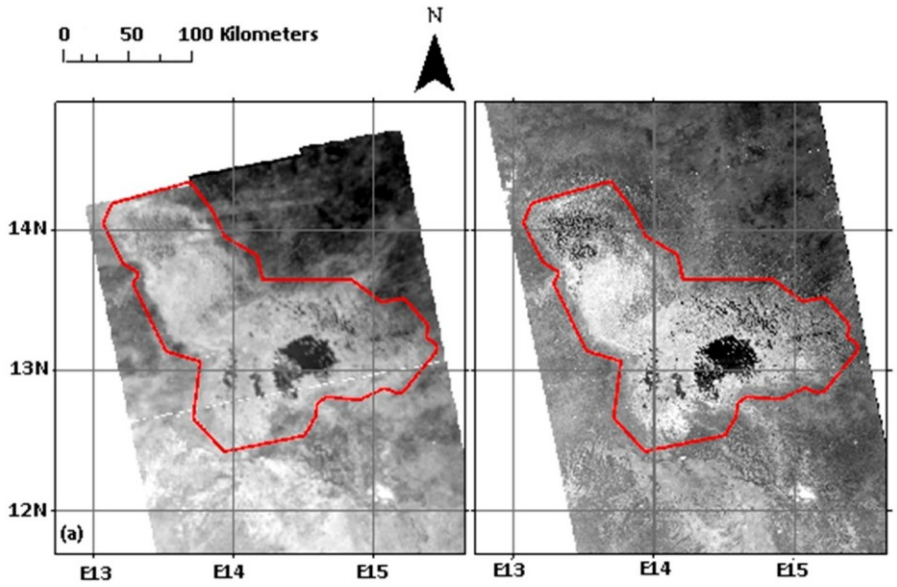

Figure 1.5. Example ESA Sentinel-1a C-band radar acquisitions, (**a**) wet season (16 July 2015) (**b**) dry season (9 April 2015).

Table 1.2 Lake Chad area calculations by subdivision of lake for 18 available pairs of ESA Sentinel-1a C-band radar and corresponding NASA MODIS Land Surface Temperature (LST) data.

	Average Total Surface Water Area Radar (sq. km)	Standard Deviation Radar (sq. km)	Average Total Surface Water Area LST (sq. km)	Standard Deviation LST (sq. km)	Percent Difference
Southeast Lake Chad	3472	312	4529	422	31
North Lake Chad	4954	811	4115	1337	−19
South Lake Chad	5029	192	5041	197	0.3
Total Lake Chad	13,455	1092	13,685	1354	2

There is a substantial publication record (e.g., Wilusz et al, 2017, Hess et al., 2003, White et al., 2015, Sass and Creed, 2008) for the use of radar data for mapping wetlands including flooded vegetation. Wilusz et al., 2017 found that "low resolution C-band SAR imagery shows promise for long term study of Sudd wetland flood dynamics." From a remote sensing perspective, the Sudd and Lake Chad have many similarities, and application of a successful technique in one area should encourage trial of that technique in the other. Radar has the advantage over LST of a relatively extensive history of use for mapping flooded vegetation. According to White et al., 2015, "SAR (Synthetic Aperture Radar) has many characteristics that make it ideal for mapping and monitoring water and wetlands over time." According to Henderson and Lewis, 2008, "What is evident throughout the recent literature is that multidimensional radar data sets are attaining an accepted role in operational situations needing information on wetland presence, extent and conditions." According to Guo et al., 2017, "Because of the strength of penetrating vegetation canopy and acquiring ground information all day without the limitation of clouds, radar data . . . are uniquely suited to identify and monitor changes of soil moisture, (and) flooding . . . in wetlands." Given the relative maturity of the radar approach vs. the LST approach, we decided to use the differences between radar and LST-based estimates for the three subdivisions to derive

appropriate correction factors to adjust the LST-based total surface water area time series.

Figure 1.6 shows an example comparison of the LST and radar-derived water classifications. Note the spatial differences despite relatively close total surface water area estimates for these images. The example LST image (Figure 1.6a) contains close to 12,300 square kilometers of total surface water area, while the corresponding radar image (Figure 1.6b) contains approximately 12,100 square kilometers of total surface water area, a difference of approximately 2 percent.

After adjusting the MODIS LST-derived lake area results using the differences with radar and then comparing the adjusted MODIS LST lake area results with the Leblanc et al., 2011 results using Meteosat LST, we found a low difference (our data was approximately 3 percent higher) during the period of overlap (dry season portion of March 2000–May 2001); see Figure 1.7.

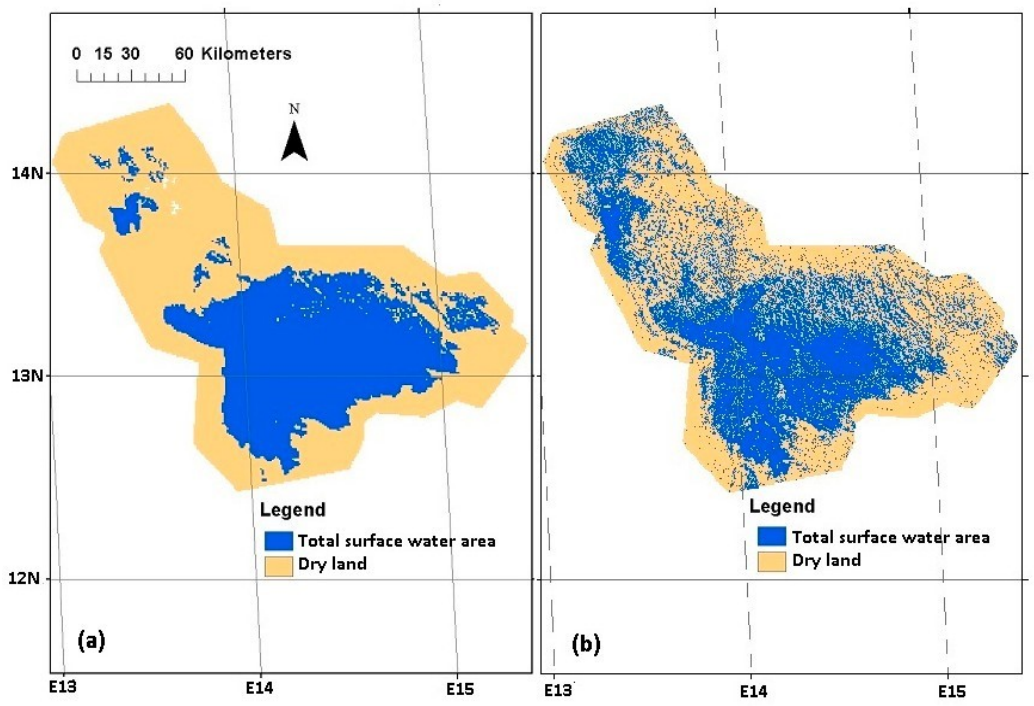

Figure 1.6. (**a**) Example NASA MODIS Land Surface Temperature (LST)-derived dry season water classification (31 October 2016–7 November 2016) (**b**) Example ESA Sentinel-1a C-band radar-derived dry season water classification (5 November 2016).

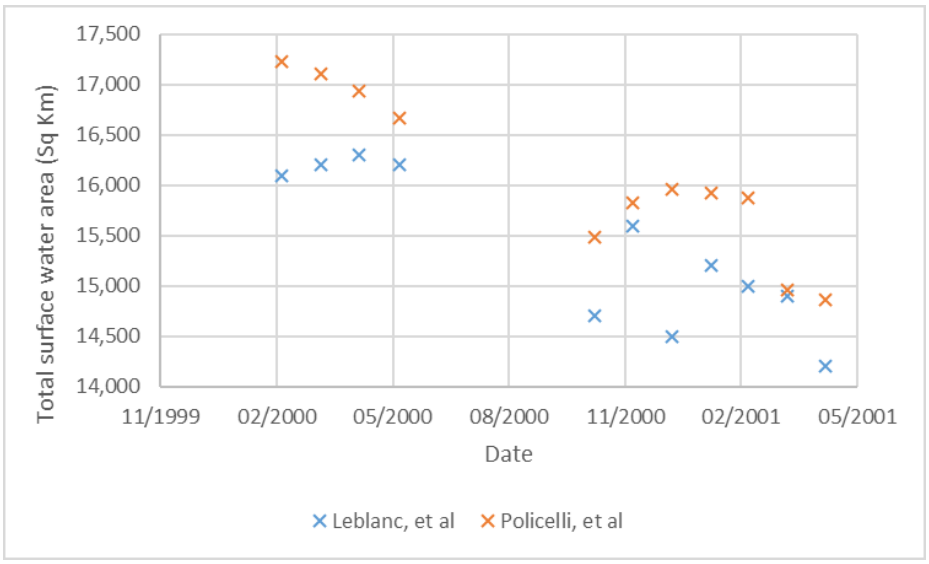

Figure 1.7. Comparison of Lake Chad total surface water area estimates using NASA MODIS Land Surface Temperature (LST) from this study with results from Leblanc et al., 2011.

Based on the very similar results during the period of overlap, we concluded that it was appropriate to bias adjust the Leblanc et al., 2011 data, and present a single integrated time series of the two data sets approximately doubling the period of lake total surface water area time series. In Figure 1.8, we plot the mean, maximum and minimum annual lake areas for each year (values are monthly), along with the mean, maximum, and minimum trend lines. Note that a given year represented on the graph corresponds to the dry season (November through May) starting in that year.

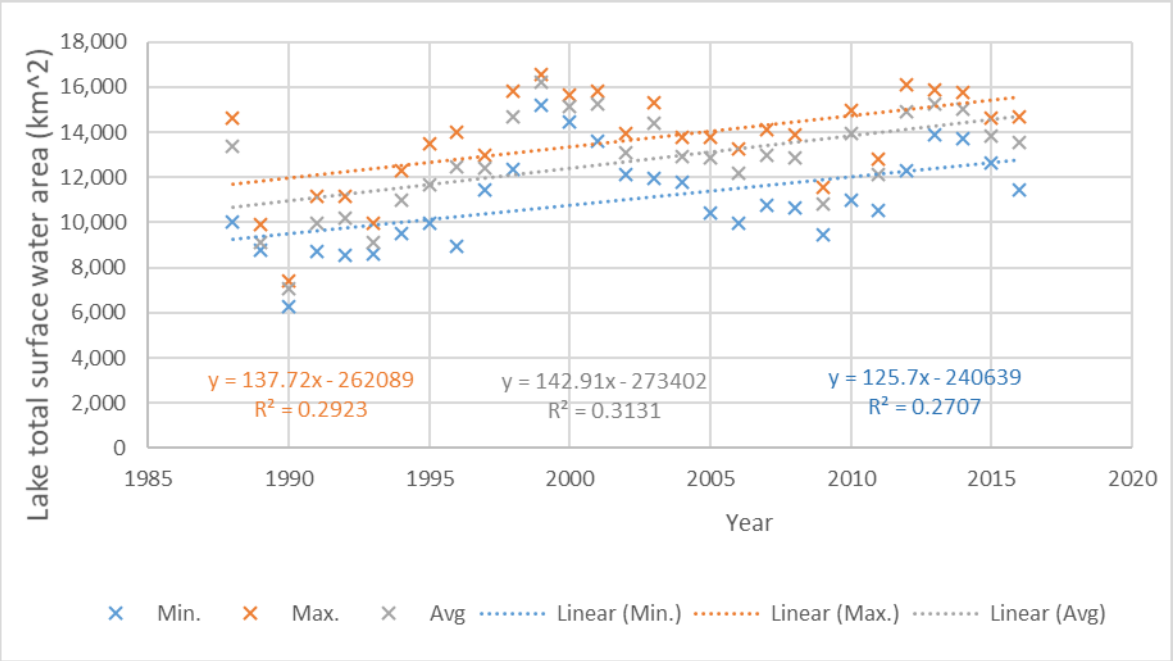

Figure 1.8. Annual mean, maximum, and minimum Lake Chad dry season total surface water area time series composite from Leblanc et al., 2011 and the research for this paper. Each data point represents a full month. Trend lines are included.

The general trend for the average total surface water area of the lake (Figure 1.8) has been an increase of approximately 143 km^2 per year (slope of the average trend line). The R-Square value of the average trend line is 0.31 indicating high variability relative to the linear trend line. The slopes and the R-Square values are slightly lower for the maximum and minimum trend lines. A sinusoidal fit to the data is suggested by Figure 1.8 (with periodicity between 11 and 13 years) and may be the result of large-scale climate oscillations. The El

Nino phase of ENSO has a known influence on Lake Chad water level variability (Okonkwo et al., 2014). However, "a much deeper understanding of the effect of other oceanic conditions like Atlantic Multidecadal Oscillation (AMO), Indian Ocean, and Mediterranean (oscillations) at different time-scales on Sahel precipitation is needed for a complete picture" (Okonkwo et al., 2014) of Lake Chad level variability.

The 25th percentile of total surface water area is approximately 11,700 square kilometers, the 50th percentile is approximately 12,900 square kilometers, and the 75th percentile is approximately 14,400 square kilometers. The time series exhibits a sharp decrease in the first two years, followed by a rise from 1990 to 1999, and then declining to 2009, rising to 2012, and a short, moderate decline since then.

The data show that, for the dry season, November is the month with the smallest lake total surface water area on average and the highest lake total surface water area occurs in March on average (Table 1.3). There is considerable variability for each month.

Table 1.3 Monthly average Lake Chad total surface water area for dry seasons **1**988–1989 through 2016–2017.

	November	December	January	February	March	April	May
Average Area (sq. km)	10,834	12,067	12,946	13,306	13,410	13,282	13,060
Standard Deviation (sq. km)	2090	2201	2270	2357	2361	2287	2284

During the 2-class unsupervised classification of the MODIS LST data, we found that there was a substantial difference in the mean temperature between the two classes. As can be seen from Figure 1.9, the mean temperature of the dry land class ranges between 5 and 15 degrees Kelvin above the average of the surface water class. This temperature difference provides a level of confidence that the two classes are sufficiently different to separate clearly. The maximum of the average surface water temperature was 310 degrees Kelvin (17–24 May 2010), and the minimum of the average surface water temperature was 292 degrees Kelvin (9–

16 January 2002). The maximum of the average land surface temperature was 324 degrees Kelvin (17–24 May 2010), and the minimum of the average land surface temperature was 300 degrees Kelvin (1–8 January 2015). Again, only dry season data was used because of cloud contamination, data loss, and ambiguities between wet soil and inundated areas during the wet season.

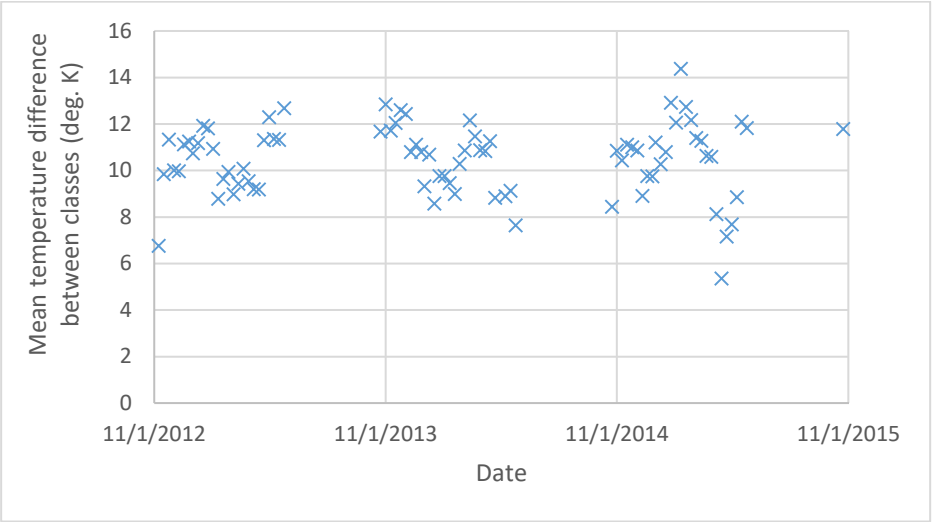

Figure 1.9. Time series of mean temperature difference between classes (dry land surface temperature—water surface temperature) in the unsupervised classification of Land Surface Temperature (LST) data.

For the adjustment of the MODIS LST-derived total surface water area due to spatial disagreement with the radar data, we found that despite significant adjustments to the sub divisions of the lake, the average lake total surface water area was not changed greatly relative to the initial LST results. The average change of the total surface water area after adjustment of the sub divisions was about −1 percent, while the maximum change was about −8 percent. Figure 1.10 presents a time series of the change. Both the time series in Figure 1.10 and in Figure 1.8 have a down-up-down pattern of approximately the same shape since 2000.

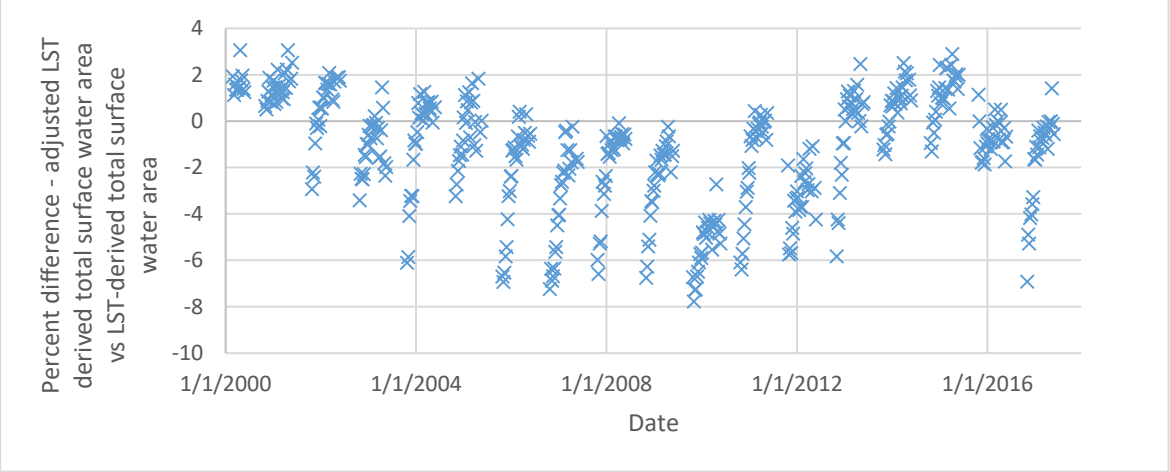

Figure 1.10. Percent difference between adjusted MODIS Land Surface Temperature (LST) -derived Lake Chad total surface water area and initial total surface water area. The results retain a strong seasonal signal from the source LST data.

1.5 Discussion

Use of the NASA MODIS Land Surface Temperature product has allowed us to extend the time series of Lake Chad's total surface water area by about 15 years, updating and approximately doubling what was previously available. Having this time series helps us answer some fundamental questions about the dynamics of the lake including "what is the average total surface water area of the lake?" and "is the lake shrinking or growing?"

There are many challenges associated with estimating the total surface water area of Lake Chad; chief among them are the apparently extensive amount of flooded vegetation, which cannot be identified as containing water using optical remote sensing instruments. Leblanc et al., 2011, citing work by Lemoalle, 2004 and Carmouze and Durant, 1983, subscribe to the idea that, "the transition from an 'Average' to a 'Small' Lake Chad in 1973 . . . was accompanied by the development of aquatic vegetation which now dominates the inundated area of Lake Chad". To get an accurate accounting of the lake's total surface water area, it is necessary to measure both the open water and the area covered by aquatic or "flooded" vegetation. Any approach that ignores this is bound to significantly underestimate the total

surface water area of the lake. We have chosen to use LST and radar remote sensing datasets, as these approaches are inherently able to retrieve information beneath modest canopy coverage. It appears that surface water area under vegetation cover is often left out of consideration of the area of Lake Chad. The main cause of this oversight is likely the challenge of using remote sensing techniques to estimate the area of flooded vegetation associated with the lake. Though they do not provide any detail on their methods, the World Lakes Database of the International Lake Environment Committee's estimates that Lake Chad covers just 1540 km^2 is likely an example of this.

Other challenges include (1) the lack of ground-based measurements of the Lake Chad water extent, which precludes validation of the remote sensing approach using in situ data; and (2) the relatively coarse resolution of the LST data available, which makes it difficult to get accurate areas for the small bodies of water associated with the lake in northern and southeastern Lake Chad.

The results of Leblanc et al., 2011, using Meteosat-based LST compare well with the overlapping period of adjusted MODIS LST-based results from this study; the Meteosat data is three percent lower on average. This similarity is to be expected because similar methods were used, however different LST data were used for the two sets of results, and Sentinel-1a C-band radar data were used to adjust the spatial biases in the MODIS LST data used in this study. The study by Leblanc et al., 2011 did not compare their results with other remote sensing approaches, though they did have one in situ observation. Additionally, the resolution of the LST data (1 km) was higher for this study than for the Leblanc et al., 2011 study (5 km), which should tend to give this study a better measurement of total surface water area. Atmospheric conditions such as clouds and dust have the potential to impact measurements of total surface water area for both the MODIS and Meteosat-based LST approaches, though this has been mitigated by several methods including the use of dry-season data only and monthly

averaging of data without significant cloud coverage.

According to Bouchez et al., 2016, Lake Chad reached 14,000 square kilometers in April 2013. This is within close to ten percent of our figure of 15,600 square kilometers for the same month.

The results from Birkett, 2000 did not compare well with the results from this study. In general, the results from the current study are 2 to 3 times higher than the peak areas from Birkett, 2000. The study by Birkett, 2000 used near-infrared bands to detect water, though this method will only detect open water. While Birkett, 2000 notes that some surface water area may be "masked by perimeter vegetation", she does not mention the possibility of extensive masking by aquatic vegetation as cited by Leblanc et al., 2011, and her values of total surface water area are considerably lower than for Leblanc et al., 2011 and this study.

Because the reports of long term changes to Lake Chad described in the Introduction cover different time spans, they cannot be directly compared to our results, though it is worth mentioning that Grove, 1996; UNEP (a), 2006; and Lemoalle et al., 2012 show a large shrinking of the lake, and the results of Leblanc et al., 2011 and this study show a modest net growth of the lake. On the other hand, indications of increased surface water area, rainfall, lake elevation, and flow to the lake by Birkett 2000; the Lake Chad|World Lake Database-ILEC; and Biasutti and Giannini, 2006 are all consistent with a net growth of the lake during the period of our research.

As an example of model performance compared with our observation-based approach, Gao et al., 2011uses the Variable Infiltration Capacity (VIC) hydrological model (Bowling and Lettenmaier, 2009) to estimate the total surface water area of Lake Chad from 1952 to 2006. From the late 1980s to 2006, they show a net rising trend in lake total surface water area, as does this study for the same period. In 1990, Gao et al., 2011 calculates a peak area of approximately 5,000 square kilometers (compared to our value of 7,400 square kilometers); in

2000 they calculate a peak area of approximately 12,500 square kilometers, (compared to our value of 15,600 square kilometers) and in 2005 they calculate a peak area of approximately 10,000 square kilometers (compared to our value of 13,800 square kilometers). While the absolute values are very different, the trends are similar. The modeling approach has the advantage that total lake surface area can be forecast and wet season total lake surface area can be calculated. On the other hand, we expect observations of total lake surface area to be more accurate than calculation of area by a hydrological model, especially given the uncertainties of rainfall datasets over Africa (Sylla et al, 2013), and the complex topography of the lake area.

Wilusz et al., 2017 used only C-band radar for their analysis of the Sudd wetland flooded area in South Sudan. The radar data is not affected by clouds and can be taken during the day or night. While their results did not require adjustment, they were limited to five years of available data (compared to twenty-eight years in our study). In our analysis, we calculated total surface water area using two remote sensing methods, C-band radar and LST. The C-band radar and LST methods agree well in southern Lake Chad, which contains a great deal of open water. However, when determining total surface water area in north and southeast Lake Chad, two competing factors (i.e., penetration of canopy and spatial resolution) resulted in a difference between the C-band radar and the LST method. In north Lake Chad, where there is a large extent of vegetated water, the LST method underestimates total surface water area relative to the radar. C-band radar has the ability to penetrate vegetation canopy to some extent and detect surface water in flooded vegetation in addition to open water (Kasischke et al., 2011). While the use of unsupervised classification on LST data can identify surface water through gaps in the canopy, this method can be negatively affected by the warmer canopy even though it is moderated by the cooling effect of vegetation through transpiration and other mechanisms (Jones et al., 2011). In southeast Lake Chad, the landcover is mainly a

mix of dunes and open water. The coarser resolution of the LST method tends to classify a large area of these mixed pixels as water due to the large difference between water and land surface temperatures, which leads to an overestimate of surface water area in this region relative to the radar. We adjusted for these under- and over- estimates by using a correction factor for each of the three sub-divisions for the data from this study and then used the adjusted data to bias correct the data from Leblanc et al., 2011.

Extension of the Lake Chad area time series can be continued using MODIS LST as long as either MODIS on the NASA Terra or Aqua satellites is operating. However there is now another option with the LST product from the VIIRS sensor on the NASA Suomi NPP satellite, and soon to be available from the VIIRS sensors on the NOAA JPSS series of operational satellites. The VIIRS sensor provides LST data at a higher resolution (0.75 km) than the MODIS sensor or the Meteosat-based sensor (Islam et al., 2017).

1.6 Conclusions

In this study, we compared the Land Surface Temperature (LST) method and the radar method of measuring Lake Chad's total surface water area (open water plus flooded vegetation), assumed that the widely used, higher resolution radar method is more reliable, and adjusted the longer LST record using data from the radar method. We used 8-day NASA MODIS LST data from March 2000 to May 2017, ESA Sentinel-1a C-band radar data acquired from April 2015 to May 2017, and Lake Chad total surface water area data from a previous study for November 1988 to May 2001.

To identify the total surface water area of Lake Chad, we examined LST and radar datasets from which we derived similar overall areas, although with significant differences in the spatial coverage of each. The comparison of the LST and radar datasets likely suffered from the fact that it was necessary to use 8-day MODIS LST data to effectively clear clouds and provide complete datasets, as compared to the use of single day radar data, the fact that

the radar data are much higher resolution (100 m resampled for radar, and 1 km for the LST), and the ability of radar to penetrate modest canopy coverage. C-band radar products from Sentinel-1a are relatively new, and there is no close analog on other platforms that was readily available for this study, with the exception of Sentinel-1b, which has an even shorter data record.

The availability of radar data from Sentinel-1a for a portion of the LST record enabled us to adjust the LST-derived total surface water area estimates and extend the existing total surface water area record for Lake Chad. A picture has emerged of the past 28 years of Lake Chad's total surface water area that is generally increasing, at an average rate of 143 square kilometers per year and with a great deal of variability (described above). For the dry season of 1988–1989 through the dry season of 2016–2017, we find that the maximum monthly average total surface water area of the lake was approximately 16,800 sq. km (February and May 2000), the minimum monthly average total surface water area of the lake was approximately 6400 sq. km (November 1990), and the average of the total monthly surface water area was approximately 12,700 sq. km. The 25th percentile of total surface water area was approximately 11,700 square kilometers, the 50th percentile was approximately 12,900 square kilometers, and the 75th percentile was approximately 14,400 square kilometers.

This research has addressed important questions about the size and trend of Lake Chad's total surface water area. Future efforts at mapping and calculating the area of Lake Chad would greatly benefit from in situ measurements, as well as the continuing radar and LST records.

CHAPTER 2

A predictive model for Lake Chad total surface water area using remotely sensed and modeled hydrological and meteorological parameters and multivariate regression analysis

2.1 Introduction

Lake Chad is a shallow, endorheic lake in the Sahel region of west-central Africa shared by Chad, Nigeria, Niger, and Cameroon. There have been numerous hydrological models developed for Lake Chad. Each of these has limitations relative to the statistical model for lake area we present here.

Bader et al. (2011) developed a hydrological model that simulates the water level in the northern pool, southern pool, and archipelago using riverine and direct rainfall inputs to the lake. It also estimates total water area for each of the pools. According to (Lemoalle et al., 2012), the model results correspond well with satellite measurements of northern pool surface water area and with satellite measurements of the total surface water area from 1980 onward, though these results are not quantified. One disadvantage of this model is that it requires input of the Chari River and Komodougu-Yobe River discharges, data that is not publicly available.

Coe and Foley (2001) report the results of a hydrological model of Lake Chad. They describe a model with "good agreement with the inferred lake area" during simulations for the years 1954 to 1967. The "inferred lake area" is not a direct measurement of lake area, but rather is derived from a relationship between lake area and lake level. It is important to note that the hydrology of Lake Chad changed significantly in the 1970's during its transition from "Normal Lake Chad" to "Small Lake Chad" and the model, based on a coarse (10 km resolution) digital elevation model, may not be adequate to define the lake after this transition.

Gao et al. (2011) developed a hydrological model of Lake Chad. They compared images of the lake extent from the model with images derived from remote sensing. Three image pairs were shown, for October 31, 1963; December 25, 1972; and January 31, 1987. Each pair of images from the two earlier dates (before the transition from "Normal Lake Chad" to "Small

Lake Chad") looked quite similar, though no numerical value was provided. The model-observation pair for the post transition period did not look very similar. This raises the question of the utility of the model for producing lake area in the current, post transition period.

Lemoalle (2004) developed a crude expression for Lake Chad surface area based on a simplified water balance model and described it as a "first approximation." That model assumes no seepage from the lake and requires knowledge of the streamflow to the lake, which as previously noted is not publicly available. Delclaux et al. (2008) developed a hydrological model of the Lake Chad Basin, however the results they presented included streamflow and elevation, but not surface area.

Coe and Birkett (2004) used upstream measurement of river height along with in-situ stream flow and gauge height to estimate river discharge 500 km downstream and wet season height of Lake Chad, greater than 600 km downstream. Their method, though, clearly relies on hard-to-obtain in-situ measurements and does not include lake area.

The first objective of this paper is to assemble and examine a set of satellite- and model-based data for the southern Lake Chad Basin relevant to developing a statistical model for the area of the lake during its flooding season. This data set includes time series of satellite- and gauge-based precipitation and modeled ET for the southern part of the basin, modeled lake ET data, satellite-based lake elevation data, and satellite-based estimated lake total surface water area. Given the limitations of the existing models described above, the second objective is to develop a predictive statistical model for total lake surface water area using regression methods on the data set. The regression method includes backward elimination variable selection and a Leave One Out Cross Validation (LOOCV) analysis to optimize the resulting statistical model.

2.2 Study Area

The Lake Chad basin is approximately 2.5 million square kilometers, about eight percent of the African continent, and the largest endorheic basin in the world (Gao et al., 2011). Lake Chad is the terminal lake of this basin. The northern part of the basin lies within the Sahara and does not generate runoff that reaches Lake Chad (Delclaux et al., 2008). For this reason, we work with the southern part of the basin (figure 2.1).

Fig. 2.1 Southern Lake Chad Basin (white), lake, and major rivers (blue)

The lake's average depth varies between 1.5 and 5 m. Any change in lake volume translates to a substantial change in lake shoreline and area ("Lake Chad flooded savanna", World Wildlife Fund, no date, https://www.worldwildlife.org/ecoregions/at0904).

In the 1960's the lake's area was on the order of 25,000 sq. km.; in the mid-1980s its area was reported to be about one tenth of that size (Grove, 1996), though it is not clear if that includes flooded vegetation. If one includes flooded vegetation, the lake's annual peak area for 2017 is estimated at close to 14,700 sq. km (Policelli et al., 2018a). Figure 2.2 shows the evolution of Lake Chad from the time of the earliest space-based images of the lake.

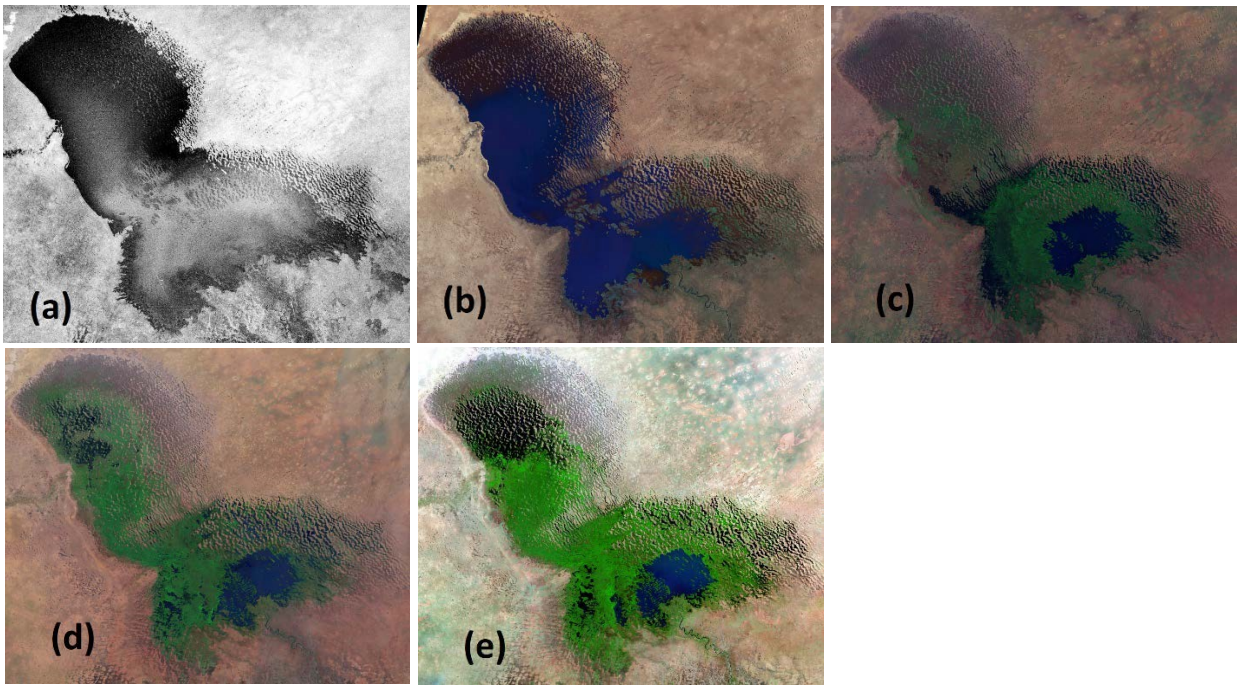

Fig. 2.2 Evolution of Lake Chad. Optical imagery from (a) 1963, Argon satellite (b) 1973, Landsat 1 (c) 1987, Landsat 5 (d) 2003, Landsat 7 (e) 2013, Landsat 8. Images provided by U.S. Geological Survey, Department of the Interior/USGS

Below about 280 m ASL, the lake separates into a southern pool and a northern pool divided by "the Great Barrier", and the southern pool separates from the eastern "archipelago" of sandy islands (Lemoalle, 2004).

The population of the lake shore is around 2 million (Magrin, 2016) and the people make a living through a combination of fishing, farming, and raising livestock (Sarch and Birkett, 2000).

"Recession farming" is an important method of farming in the region whereby farmers plant in the enriched soils following each year's flood pulse. Because of the complexity of the hydrology, it is difficult to provide farmers with information on the timing of the floods and a sense of how large the flood is going to be in any given year. This can be a serious problem for farmers who grow crops near the lake shore and periodically lose crops to flooding (Okpara et al., 2016).

According to (Sarch and Birkett, 2000), the "farming start date" at villages on the south-west shore of Lake Chad begins in mid-January to late February. It seems reasonable to conclude that predictions of lake surface area made in late November or early December could be used for agricultural decision making for locations with similar start dates.

There are a number of dams and irrigation schemes in the river basins that drain into Lake Chad, such as those of the Chari-Logone and Komadougu-Yobe river systems. However, at the large scale, they do not amount to a substantial revision of the natural seasonal hydrological patterns, which are largely determined by the West African Monsoon and the position of the ITCZ (Birkett, 2000).

The surface of Lake Chad is not flat and level; the barriers to flow from the southern pool to the northern pool and archipelago result in the water in these areas frequently being at different elevations. Additionally, the local winds and flow of water from the Chari River into the lake (addressed further in the Discussion section) combined with the complex shape of the lake lead to an evolving lake surface (Carmouze et al., 1983). Lake surface elevation time series data used in this study refer to satellite-based measurements made in the relatively small open water portion of the lake in the southern pool.

Figure 2.3 presents areas of the lake at or below selected elevations. The topographic data used to create figure 2.3 is from a 1 arc-second (~30m) resolution Digital Elevation Model (DEM) from the NASA Shuttle Radar Topography Mission (SRTM). The blue areas would correspond to lake levels (limited by the accuracy of the DEM) if the lake surface were flat and the lake filled uniformly. However, since this is not the case, the areas should only be viewed as providing context for Lake Chad landforms and hydrology.

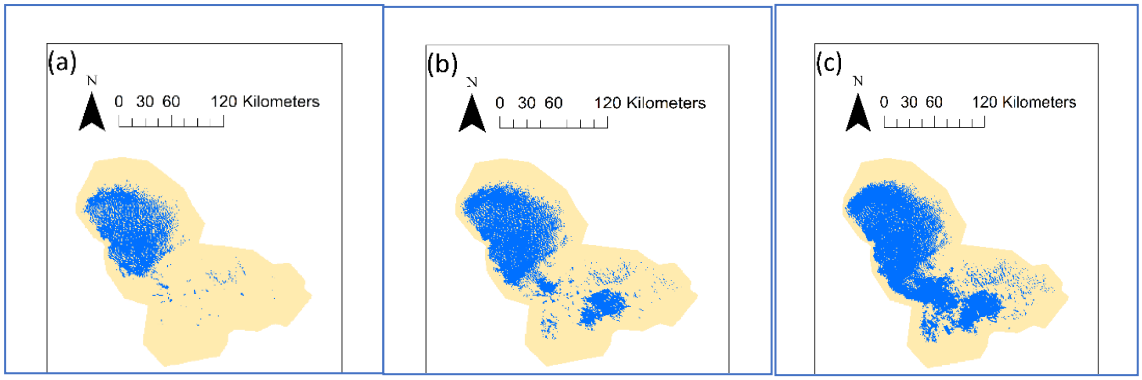

Fig. 2.3 Blue areas have elevations at or below (a) 279m ASL, (b) 280m ASL, (c) 281m ASL

According to (Leblanc et al., 2011) most of the flooded area of Lake Chad is covered by aquatic vegetation including rooted and floating plants. This area is not readily measured with optical remote sensing, but must be accounted for to get an accurate estimate of total surface water area for the lake (Policelli et al., 2018a).

Lake Chad receives 90-96% of its water from the Chari-Logone River system (Zhu et al., 2017a), with the remaining coming from smaller tributaries and direct rainfall. Most of this water arrives from such a distance that the peak lake level and lake area occur months after the rainfalls that produce them. The delay is due to the slow runoff and routing of flood water to Lake Chad from the southern portion of the basin where precipitation rates are highest (Leblanc et al., 2011). It is the reason that the Lake Chad peak level and area take place in the dry season.

2.3 Data and Methods

2.3.1 Data

The key datasets used for this research are (1) Climate Hazards Group Infrared Precipitation with Station data (CHIRPS), (2) satellite altimetry-based lake surface elevation data, (3) evapotranspiration (ET) data from the Famine Early Warning Systems Network (FEWS NET) Land Data Assimilation System (FLDAS), (4) percent of 1988-2016 lake ET

average estimates, (5) the HydroBASINS shape file for the southern Lake Chad Basin extent and (6) lake total surface water area data, described in (Policelli et al., 2018a).

2.3.1.1 CHIRPS (Funk et al., 2015) is a quasi-global precipitation dataset produced by the Climate Hazards Group at the University of California, Santa Barbara using both satellite data and rain gauge data. We used the high resolution (.05 degree x .05 degree) daily Africa rainfall dataset, which is available from January, 1981 and updated through the previous month around the third week of each month. In comparison with the lower resolution gauge-based GPCC reference precipitation product (Schneider et al., 2015), for wet seasons in Africa CHIRPS has a mean error of 79 mm per 3 months, a mean bias of 0.22 and a correlation of 0.56 (Funk et al., 2015). In comparison with other observations-based precipitation products for Africa, CHIRPS data has higher spatial resolution, better coverage of rain gauge stations, and applies improved statistical methods (Badr et al., 2016).

2.3.1.2 Lake surface elevation data are provided by the Global Reservoir and Lake Monitor (G-REALM) on the USDA Crop Explorer website ("Satellite Radar Altimetry: Global Reservoir and Lake Elevation Database," no date, https://www.pecad.fas.usda.gov/cropexplorer/global_reservoir/). Lake surface elevation data are produced from the radar altimetry satellite missions Topex/Poseidon (1992-2002), Jason-1 (2002-2008), Jason-2 (2008 to 2016), and Jason-3 (2016 to present). The altimeters have a "footprint" diameter ranging from about 200m to several kilometers depending on the target's surface roughness. Each of the altimeters used for Lake Chad elevation data have a ten-day repeat time. The accuracy of the lake surface elevation data for Lake Chad is approximately 0.29 m (Ricko et al., 2012). Lake surface elevation data are provided as the variation from the 1993-2002 mean height.

2.3.1.3 The FLDAS ET data product is based on the Noah 3.3 Land Surface Model's total ET, which is the sum of bare soil evaporation, evaporation of water intercepted by the

canopy, and transpiration, weighted by the coverage fraction of each component (McNally et al., 2017). The spatial resolution of the FLDAS ET is 0.1 degree and we are using monthly data. The FLDAS ET data is available from October 1992 to the present. FLDAS ET has been evaluated against estimates from the Simplified Surface Energy Balance (SSEBop) satellite data-based model (Senay et al., 2013). This evaluation indicates that FLDAS and SSEBop ET have significant but limited correlation ($r < 0.5$) for percentage ET variations in West Africa. According to McNally et al., 2017, it is not entirely clear why the correlation between the FLDAS-ET and SSEBop-ET is somewhat poor in West Africa, though it may have something to do with instability of the SSEBop algorithm in that area.

2.3.1.4 We estimated the Lake Chad wet season ET as a percentage of the 1988-2016 wet season average. Because most (approximately constant at nearly 90 percent by our estimation) of the lake consists of flooded vegetation, and multiple types of vegetation are present, it is a very difficult research problem to estimate the total monthly ET from Lake Chad. However, because the ratio of open water to flooded vegetation is roughly constant over time, we were able to estimate the lake ET percent of average as the ratio of the open water evaporation for the full extent of the lake to the average open water evaporation for the full extent of the lake for 1988-2016. We used the Complementary Relationship Lake Evaporation (CRLE) model (Morton, 1986) for estimates of lake open water evaporation. The meteorological forcing data for the CRLE model were provided by NOAA NCEP-DOE Reanalysis 2. The main validation work by the developers of the CRLE model was to compare model results with lake evaporation from water balance analyses for seventeen selected lakes. On an annual basis, the model results were within a maximum of seven percent of the water balance results. Monthly results suffered an unspecified degradation of accuracy (Morton, 1986).

2.3.1.5 The World Wildlife Fund (WWF) HydroBASINS (Lehner, 2013) provided the shape file for the southern Lake Chad Basin, which was used to calculate rainfall and ET for the portion of the basin that generates very nearly all of the runoff that reaches the lake. The HydroBASINS global database of basin shapes was developed using the WWF HydroSHEDS data (Lehner et al., 2011), which has approximately 500 m resolution. The HydroSHEDS product was developed using SRTM data. No validation description or accuracy assessment was found for HydroBASINS.

2.3.1.6 Lake Chad total surface water area data from the research for (Policelli et al., 2018a) were derived from (1) 1 km resolution Land Surface Temperature (LST) data from the NASA Terra satellite's MODIS sensor and adjusted using ESA C-band radar data from Sentinel-1a, and (2) total Lake Chad surface water area estimates by Leblanc et al., [2011] derived from 5 km resolution LST data from the Meteosat MVIRI sensor and bias corrected by Policelli et al., [2018a]. The LST method for estimating lake surface water area is based on the fact that the lake, including flooded vegetation, is cooler than the surrounding landscape during the day (Leblanc et al., 2011). Monthly average area was used for this research. This data was produced for the 1988-1989 dry season through the 2016-2017 dry season. MODIS LST data with cloud cover greater than five percent were not used in the development of the lake area data. The validation done for this data was comparison of the two datasets used to create the lake area time series. The estimated lake areas for the two products during the period of overlap were within approximately three percent of each other.

2.3.2 Methods

Monthly precipitation and ET were calculated for the southern portion of the basin from October 1992 to May 2017 using the HydroBASINS shape file for this area. The Lake Chad total surface water area time series was then checked for correlation with P–ET using a series of time lags to find the peak correlation. It was expected that net precipitation (P-ET) would

be more closely correlated to lake area than either of the components. Similarly, the total lake surface water area was checked for correlation with the lake elevation data, and it was expected that a close correlation would exist between these variables (Busker et al., 2018). Additionally, the total lake surface water area was checked for correlation with the lake elevation data, the precipitation data and the ET data for the southern portion of the basin, the lake ET percentage of 1988-2016 average lake ET, and the previous year's total lake surface water area.

Next, a multivariate regression analysis was performed using the datasets to establish equations linking total surface water area for a given month to one or more of the other (independent) variables. In order to find the best relationship between the lake area and the independent variables, we used several methods of regression: 1st order linear regression, 2nd and 3rd order polynomial regression, and the linear-log method of regression. We also used the backward elimination method of variable selection to optimize the equations. To mitigate the risk of overfitting the data, we used the "rule of thumb" of ten data points for each variable included in the final equation (Harrell et al., 1996), except for 1st order linear regression, in which case as few as two data points for each variable included is permitted (Austin and Steyerberg, 2015). However, we did not use less than six data points for each variable in our 1st order linear regression analysis.

The current year's total surface water area for each month during the dry season was the dependent variable. The independent variables were (1) total wet season precipitation for the southern Lake Chad Basin, (2) total wet season ET for the southern Lake Chad Basin, (3) wet season lake ET as a percentage of the 1988-2016 average lake ET, (4) November (typically the highest) variation from the 1993-2002 mean lake surface height, and (5) the total surface water area of the given month for the previous year. A Leave One Out Cross Validation (LOOCV) was performed for the regression analysis, in which one data point was left out, the

equation was generated using regression, and the equation was evaluated for the one left out data point. This was repeated for each yearly data point and an average absolute value of the percent error was determined for the total dataset. For comparison, the average absolute value of the percent error was also determined using the average total surface water area for a given month as the prediction, and using the previous year's area as the prediction for a given month.

The study covered the time period from October 1992 to May 2017 which is the intersection of the period of available FLDAS evapotranspiration data and the available total lake surface water area data. Three years (2006-2008) were excluded from the study because of insufficient lake surface elevation data.

2.4 Results

2.4.1 Datasets

Total monthly precipitation and ET for the southern portion of the Lake Chad Basin were calculated using CHIRPS and FLDAS, respectively. Figure 2.4.a. shows the total monthly precipitation and ET for October 1992 through May 2017. The trend lines indicate essentially no change over this time period. Figure 2.4.b. shows the average monthly distribution of the precipitation and ET for the southern portion of the basin for October 1992 through May 2017. June through October is usually considered the wet season and November through May is considered the dry season (figure 2.4.b and Leblanc et al., 2011).

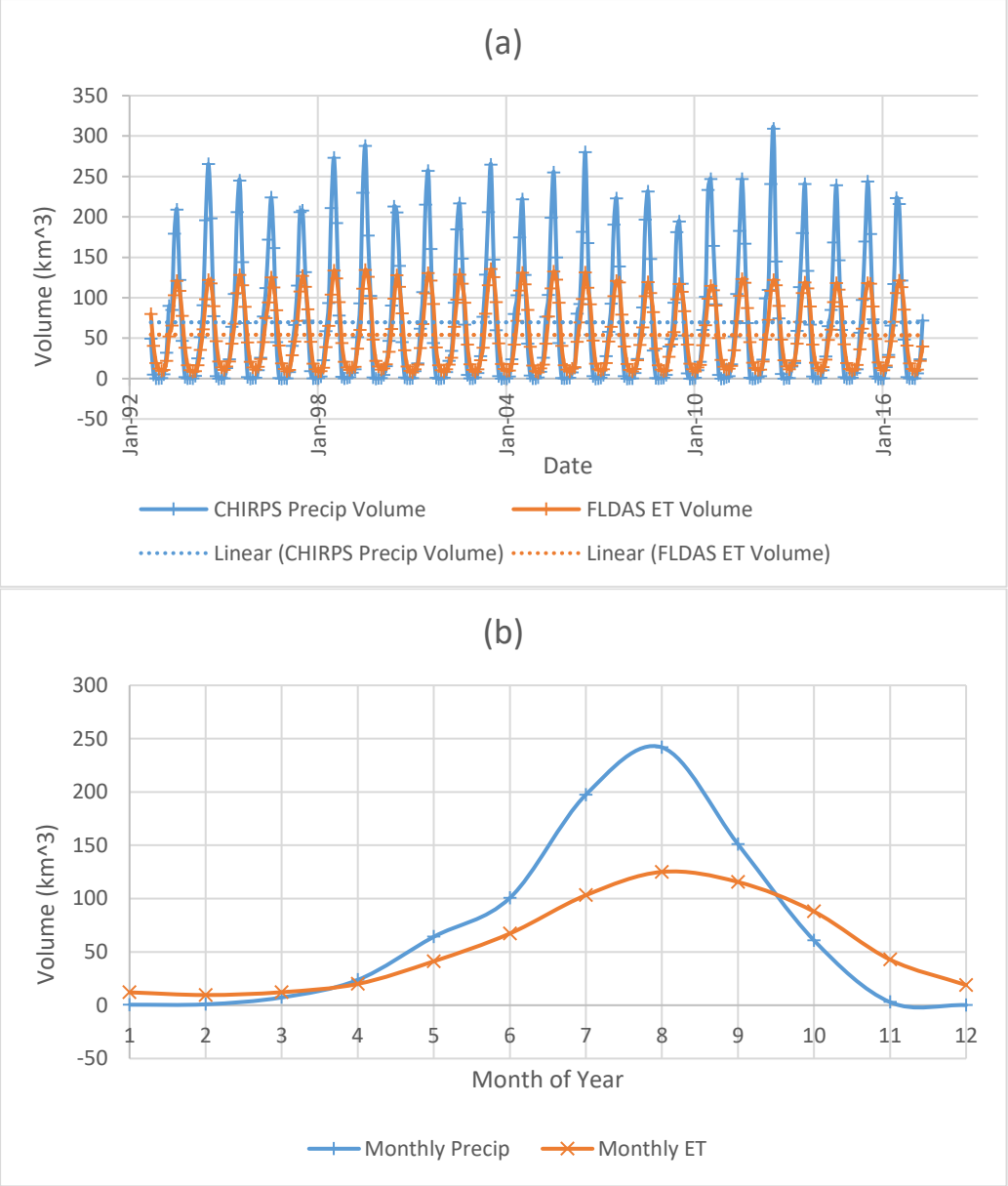

Fig. 2.4 a. monthly precipitation and ET in the Southern portion of the Lake Chad Basin b. average monthly precipitation and ET in the Southern portion of the Lake Chad Basin

Figure 2.5 shows the percent of Lake Chad wet season average ET from 1988 to 2016. The data exhibits an oscillatory behavior with a multi-year cycle and the trend is essentially flat.

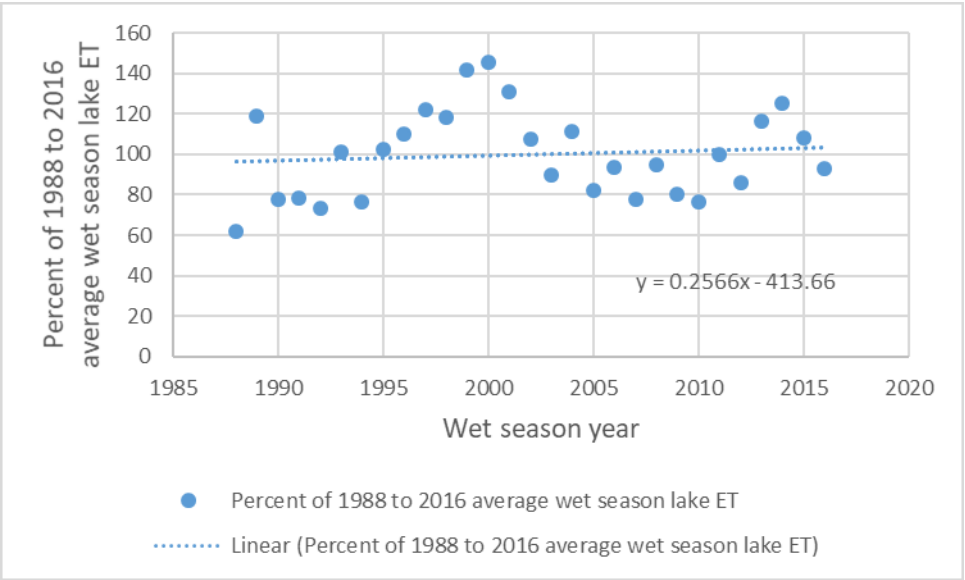

Fig. 2.5 Percentage of 1988 to 2016 average wet season lake ET

Figure 2.6.a. shows the lake elevation anomaly relative to the 1993-2002 mean level for October 1992 to May 2017. The trend line for July (the only month with complete data; not shown) shows a slight level of decrease with high variability. Figure 2.6.b. shows the average monthly lake elevation anomalies with respect to the 1993-2002 mean level for October 1992 through May 2017. Note that the average level is highest in November (during the dry season) and lowest in June (during the wet season).

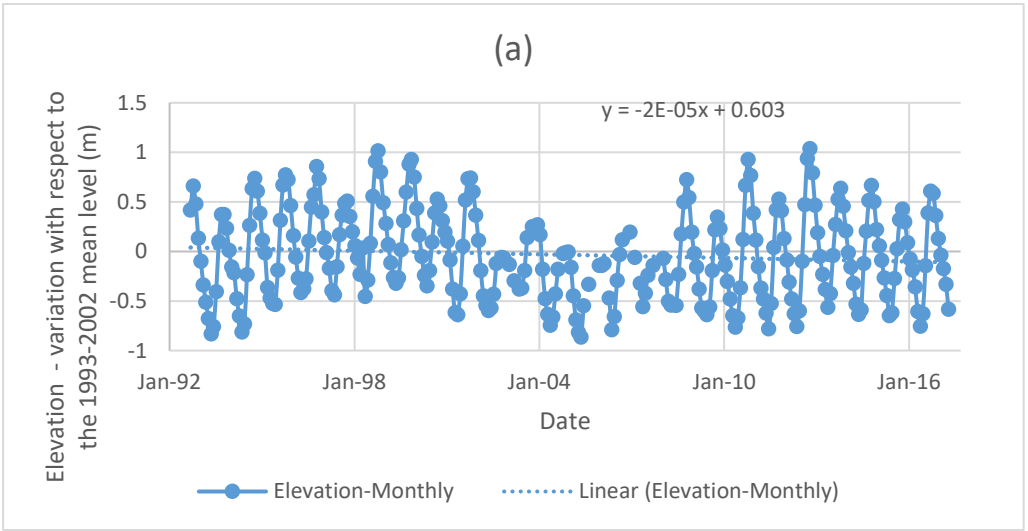

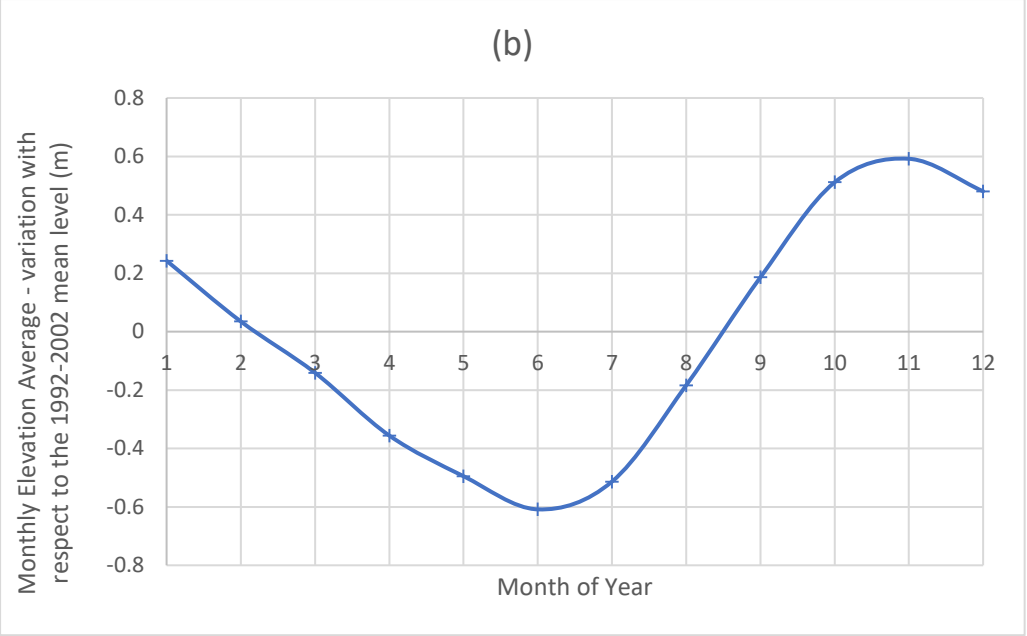

Fig. 2.6 a. lake elevation anomaly relative to the 1993-2002 mean level

b. average monthly lake elevation anomaly relative to the 1993-2002 mean level

Figure 2.7.a. presents the annual average dry season surface water area for Lake Chad from November 1992 through May 2017. As expected, the pattern of the graph is similar to that of the graph of Lake Chad percentage of 1988 to 2016 average wet season lake ET (figure 2.5). The trend line shows an average increase of approximately 82 square kilometers per year in lake area over this period. Wet season data was not considered suitable for calculation of water extent because of cloud coverage and the fact that the LST method cannot distinguish well between soil moisture and flooded areas (Policelli et al., 2018a). The total surface water area includes both open water and flooded vegetation. Figure 2.7.b. presents the average dry season monthly total surface water area for Lake Chad from November 1992 through May 2017. While the peak water elevation occurs on average in November, the peak total surface water area occurs in March on average. The peak total surface water area is not a sharp peak; the two antecedent and two following months are not far from the maximum.

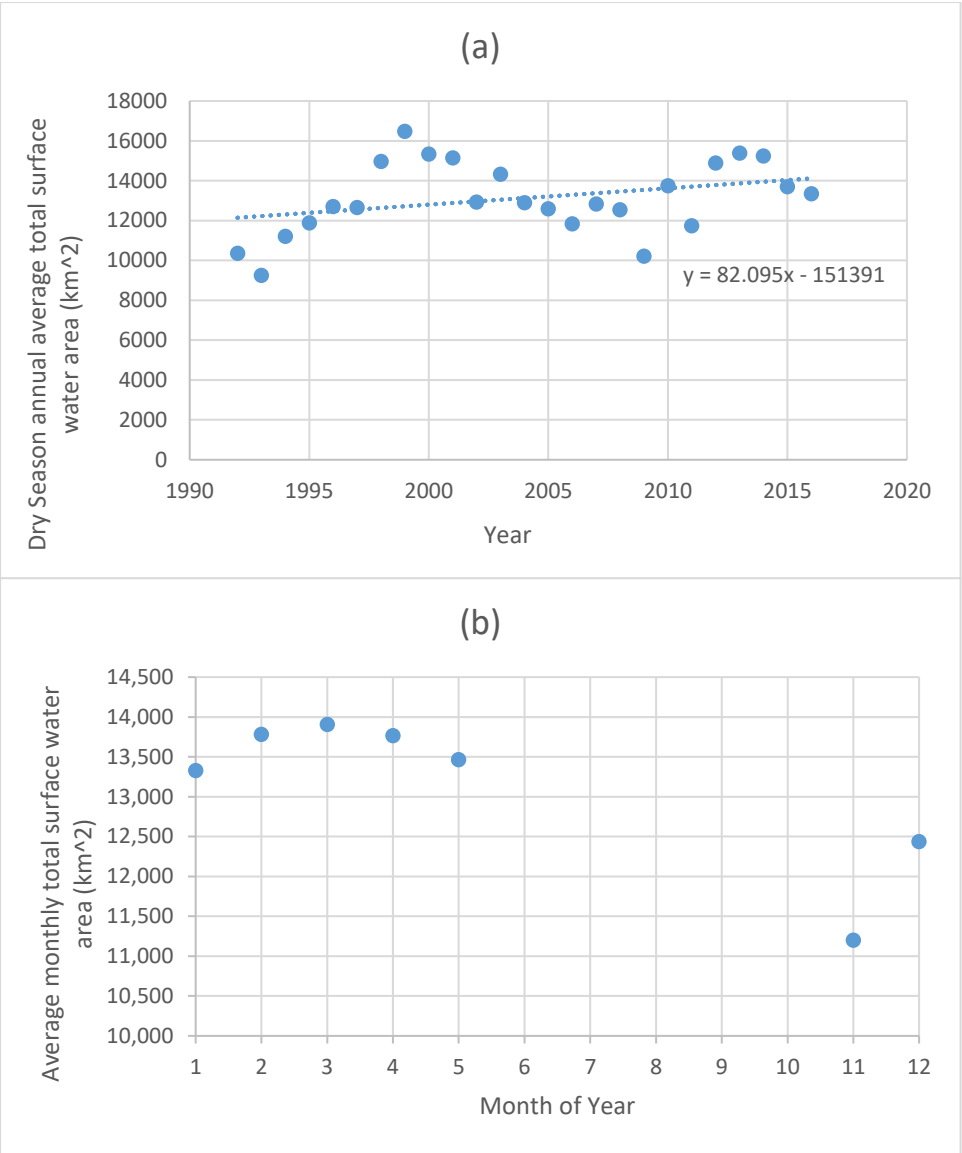

Fig. 2.7 a. average annual dry season water extent for Lake Chad b. average monthly lake water area for the dry season (November 1992 through May 2017)

2.4.2 A predictive model for Lake Chad total surface water area

During this part of the research, we asked the question: "for a given month, how well can we predict the total surface water area of Lake Chad"? To address this question, we investigated regression of the data to generate equations linking the independent variables to the dependent variable. Specifically, we looked at 1st order linear equations (Equation 1), 2nd order polynomial equations (Equation 2), 3rd order polynomial equations (Equation 3), and linear-log equations (Equation 4).

Equation 1: $A = a + b \cdot ETws + c \cdot LakeETws + d \cdot Pws + e \cdot H + f \cdot A_-$

Equation 2: $A = a + b \cdot ETws + c \cdot ETws^2 + d \cdot LakeETws + e \cdot LakeETws^2 + f \cdot Pws + g \cdot Pws^2 + h \cdot H + j \cdot H^2 + k \cdot A_- + m \cdot A_-^2$

Equation 3: $A = a + b \cdot ETws + c \cdot ETws^2 + d \cdot ETws^3 + e \cdot LakeETws + f \cdot LakeETws^2 + g \cdot LakeETws^3 + h \cdot Pws + j \cdot Pws^2 + k \cdot Pws^3 + m \cdot H + n \cdot H^2 + p \cdot H^3 + q \cdot A_- + r \cdot A_-^2 + s \cdot A_-^3$

Equation 4: $A = a + b \cdot \log(ETws) + c \cdot \log(LakeETws) + d \cdot \log(Pws) + e \cdot \log(H) + f \cdot \log(A_-)$

where: $A = A_{\text{Lake Chad, t}}$, $ETws = \sum_{June}^{Oct.}$ basin ET, $LakeETws = \sum_{June}^{Oct.}$ lake E/ lake $E_{\text{1988-2016 avg}}$, $Pws = \sum_{June}^{Oct.}$ basin P, $H = \text{Lake Elevation}_{\text{Nov}} - \text{Lake Elevation}_{\text{1993-2002 avg.}}$, and $A_- = A_{\text{Lake Chad, t - 1 year}}$

Figure 2.8 shows the scatter plots for each of the independent variables versus the average lake area for January.

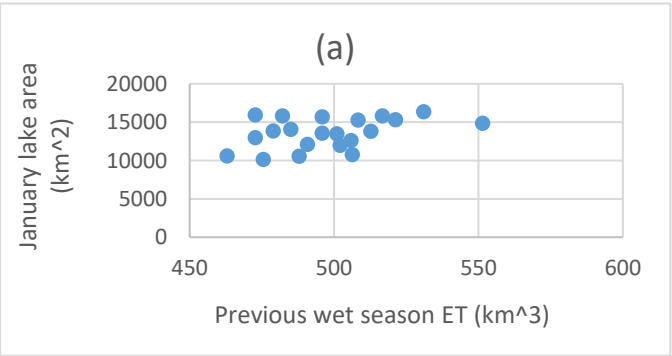

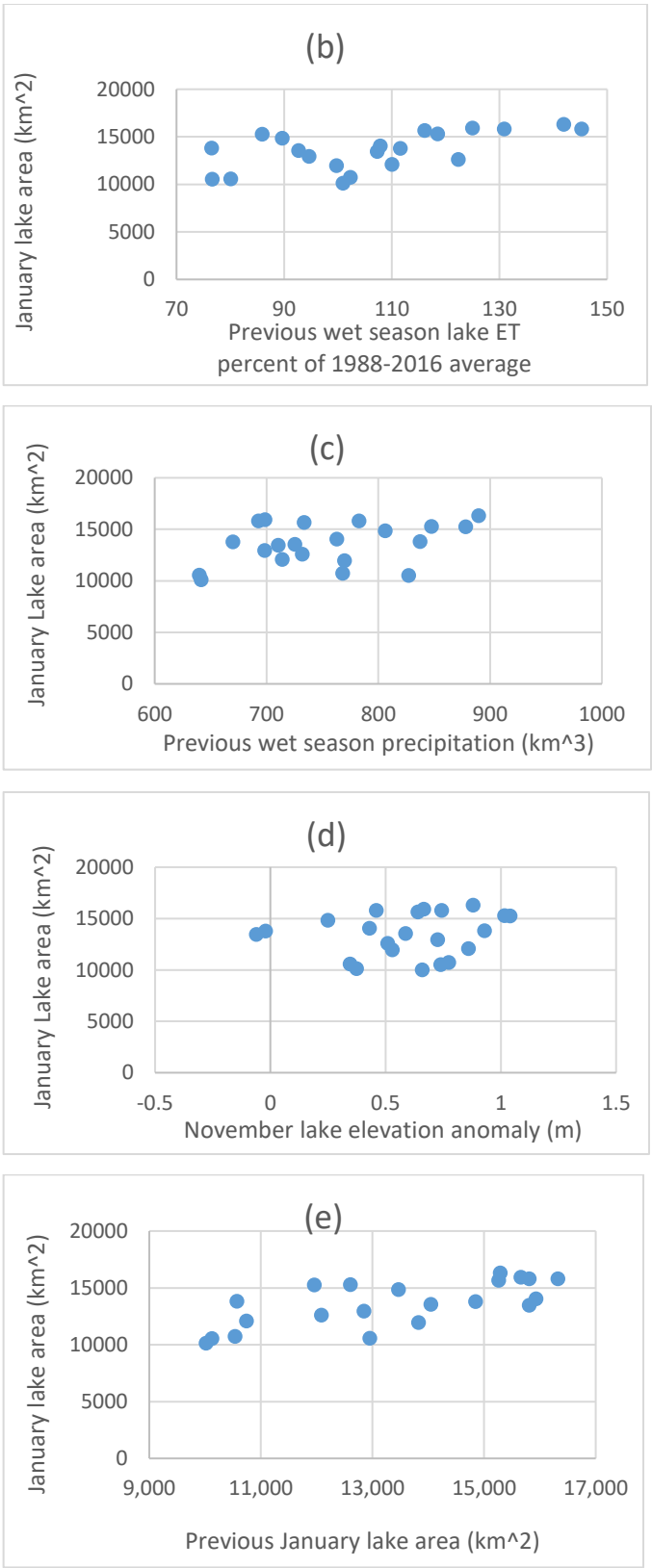

Fig. 2.8 Example (January) scatter plots for independent variables vs. lake area (a) previous wet season ET, (b) previous wet season lake ET percentage of the 1988-2016 average, (c)

previous wet season precipitation, (d) November lake elevation anomaly, (e) previous January lake area.

From our regression analysis we found that for the equation types we examined, 1st order linear equations provided the minimum average absolute percent error from LOOCV for December, February and May. For January, March and April, higher order polynomial equations provided slightly lower (between 0.7% and 1.1% lower) LOOCV average absolute percent errors. However, because of the lack of a physical explanation for some of the higher order terms (A^{-2} and A^{-3} for instance), and the marginal gain for using the higher order equations, we decided to maintain consistency across months and use optimized 1st order linear equations for all months. Linear-log solutions for the regression analysis provided higher LOOCV average absolute percent errors than the linear 1st order and polynomial solutions. The final equations are provided in Table 2.1.

Table 2.1 Equations and performance metrics for Lake Chad total surface water estimated area in terms of ETws, LakeETws, Pws, H, A-

Forecast Mo.	Lake Area Equation	LOOCV error (%)	LOOCV std (%)	Adjusted R-Squared
December	-7064.38 + 23.53 * LakeETws + 12.57 * Pws + 0.62*A-	6.05	4.60	0.78
January	-11641.42 + 25.59 * ETws + 3364.12 * H + 0.78 * A-	6.90	4.91	0.76
February	-8443.93 + 14.40 * Pws +1771.05 * H +0.76 * A-	5.25	4.66	0.80
March	-7042.42 + 14.36 * Pws + 2074.06 * H + 0.65 * A-	7.20	5.95	0.69
April	-5187.30 +12.75 * Pws + 2249.73 * H + 0.59 * A-	7.53	5.14	0.64
May	-7402.54 + 17.15 * Pws + 2203.80 * H + 0.50 * A-	7.61	6.03	0.70

The result is that this model, using three variables for each month, can be used in late November (when the precipitation data is available) to predict the Lake Chad total surface water area for December, and in early December, (when lake elevation data is available for November) the model can be used to predict the total surface water area for January through

May, with the expectation of between 5.3 and 7.6 percent error on average. This compares with (Table 2.2) the set of average absolute percent errors if the average value of the total water surface area for each month is used as a prediction,

Table 2.2 Average absolute percent error with average value used as prediction.

	average absolute % error
December	14.1
January	13.8
February	13.0
March	12.4
April	11.8
May	13.1

and (Table 2.3) the set of average absolute percent errors if the previous year's total water surface area for the given month is used as a prediction.

Table 2.3 Average absolute percent error with previous year's lake area used as prediction

	average absolute % error
December	10.0
January	9.0
February	10.6
March	12.5
April	12.8
May	15.6

For each of the months December through May, the regression approach provides a lower average absolute percent error than either the average value used as a prediction, or the

previous year's area used as a prediction. As an example, for May, the LOOCV average absolute error is 7.6%, while the error using the average May area is 13.1% on average, and the error when using the previous year's area for May is 15.6% on average. Using the average May lake area of 13,363 sq. km, these percentages are equivalent to 1017 sq. km, 1751 sq. km, and 2085 sq. km respectively.

2.5 Discussion

The lake elevation data show that the maximum average monthly elevation typically occurs in November (though on occasion in October, and once during our record in January). It is curious therefore that the maximum area typically though not always occurs in February or March. The reason for this seems to be the complex meteorology and hydrology of Lake Chad. The movement of the water in Lake Chad is influenced by both the winds and the Chari-Logone water supply. Monsoon winds drive the displacement of the southern waters toward the north, and movement begins around the northeastern end of the Great Barrier in June, at the end of the low water. The Chari-Logone flood waters begin in August and provide half of their water in October and November when the northeasterly wind known as the Harmattan drives the water back toward the southern pool. This is also when the satellite radar altimeters (which collect data over the southern pool) typically record the highest levels. During the peak of the riverine flooding, water again reaches the northern pool and also spreads into the archipelago from the south basin. Following the end of the movement of water to the north pool in January, there is a general spreading of water in the southern pool to the periphery until April. (Carmouze et al.,1983). These movements result in a complex and changing lake surface topography, and are likely the reason we find poor correlation between lake elevation and lake area.

A full parameterization of the Lake Chad system, as implemented by (Delclaux et al., 2008) using the GR_B + THMB Model, includes precipitation and reference

evapotranspiration as inputs, which are adjusted by a coefficient C, set such that the Nash coefficient is maximized for the monthly flows of the Chari-Logone River system. Precipitation is then split between a soil reservoir with maximum capacity A, and surface runoff, the amounts depending on the level of water in the soil reservoir. The soil reservoir drains through actual evapotranspiration and percolation, which generates sub-surface runoff. Elevation data from the Shuttle Radar Topography Mission (SRTM) are used for generating drainage directions and water accumulation areas. Two irrigation scenarios were modeled. Lake level data was used to validate the model results. In comparison, our model also uses precipitation and actual evapotranspiration as inputs, though only for the wet season. The timing of subsurface flow and surface flow through the river systems is simulated in our model by the delay between the wet season end and the month being forecast, and by the HydroBASINS shapefile for the southern Lake Chad Basin, which defines the limits of our representation of the lake watershed. Lake level is used in the GR_B + THMB model as memory of previous conditions, whereas the lake area for the previous year is used in our model for this purpose. Unlike the GR_B + THMB model, we do not model irrigation withdrawals; as discussed in the Introduction section, this is a small part of the overall hydrology of the Lake Chad Basin. While the GR_B + THMB model uses stream flow data to calibrate the model, and lake elevation to validate the model, we use lake area estimates for these tasks and lake elevation as an additional input parameter.

The main limitation of the model we present here is that it is not a physically-based model and may not perform well for conditions outside of those in the database we have developed. For example, we are not able to do regressions and provide predictions for wet season months because we do not have surface water area data for those conditions (Policelli et al., 2018a). Also, the performance may degrade if it is used outside of the range of areas for which the

regression models were established (8,700 sq. km – 16,800 sq. km) or when the hydrology of the lake changes substantially, such as when "small Lake Chad" transitions to "normal Lake Chad" at about 18,000 sq. km. There is no fixed date at which the model becomes unusable. However, if it is used for operational forecasting, it would be wise to regularly update the model with new data as it becomes available.

2.6 Conclusions

We have built a record of remote sensing data and model products (precipitation, evapotranspiration, lake height, and lake area) for the Lake Chad Basin and used this record to run a correlation analysis and a regression analysis. From the correlation analysis (see Appendix), we have found (1) the highest correlation between basin evaporation and total lake surface water area is 0.43 and occurs with a seven month lag, (2) the highest correlation between lake height anomaly and total lake surface water area is 0.57 and occurs with a four month lag, (3) the highest correlation between precipitation and total lake surface water area is 0.39 and occurs with a seven month lag, (4) the highest correlation between percent of 1988-2016 average lake ET and the lake total surface water area is 0.65 at zero lag time, and (5) there is a correlation of 0.63 between the surface water area and the previous year's surface water area for the same month.

Note that lake surface height is more closely correlated with total lake surface water area than is precipitation, as might be expected from a measurement further "downstream". Additionally, basin ET is closely correlated with basin precipitation as might be expected since the precipitation is the source water for ET. Finally, basin ET is slightly more closely correlated with total surface water area than basin precipitation.

From our regression analysis, we have derived a set of equations that can be used starting in late November for predicting the total surface water area of Lake Chad for a given month (except November) during the dry season. The best of these in terms of R-squared use all of

our parameters: wet season south basin precipitation (Pws), wet season south basin evapotranspiration (ETws), wet season lake evapotranspiration percent of 1988-2016 average (LakeETws), lake height variation relative to 2002-2009 (H), and the previous year's surface area for the given month (A), though we are likely overfitting the data when using all of these variables. The results of Leave One Out Cross Validation (LOOCV) testing and backward elimination variable selection show the best performing variables for December to be LakeETws, Pws and A-, for January they are ETws, H, and A-, and for February, March, April and May they are Pws, H, and A-. The regression equations perform at between 5.3 and 7.6 average absolute percent error in the LOOCV testing, and outperform predictions made using the average value for the given month or the previous year's total surface water area.

The predictions using all of the equations derived from regression in this study can be made with only remotely sensed data and model outputs; no in-situ data is required. Any improvements in the measurement of the parameters we use in this analysis would likely improve the desired end result – the prediction of the Lake Chad surface area in time to be used for agricultural decisions.

CHAPTER 3

Projections of Lake Chad total surface water area

derived by forcing a statistical model of the lake area

with results of climate simulations through the year 2100

3.1 Introduction

Lake Chad is a shallow, terminal lake in the Sahel region of Africa. Chad, Nigeria, Niger, and Cameroon share the lake. Additionally, parts of Algeria, Sudan, the Central African Republic, and a small part of Libya are included in the lake's basin, which is endorheic and has an area of 2.5 million km^2, making it the largest endorheic basin in the world (Gao et al., 2011). The northern portion of the basin reaches into the Sahara Desert and does not produce runoff that reaches Lake Chad (Delclaux et al., 2008), while the southern portion of the basin receives considerably more rainfall and is the source of the Chari-Logone River system. The Chari-Logone provides ninety percent of the water flowing to Lake Chad (Zhu et al., 2017). Because of this, we worked with data from the southern portion of the basin (Fig. 3.1), which also includes the remaining sources of lake water, specifically the Yobe River, several smaller tributaries, and direct rainfall on the lake.

Fig. 3.1 Southern Lake Chad Basin (outlined in black), major Lake Chad tributaries (in blue within the basin boundaries)

The size of Lake Chad has varied considerably over time. The lake is well known for its

dramatic decrease in size during the 1970s and 1980s. The lake had an area estimated at 25,000 km^2 in the 1960's. By the mid-1980s the lake was reportedly one tenth of that size (Grove, 1996), however it is not clear if that estimate included flooded vegetation, or only open water which is much easier to detect and measure. In this study, we used data generated for Policelli et al. [2018a] to estimate the average dry season total area (including open water and flooded vegetation) of Lake Chad from 2000-2016 at 13,450 km^2. Note that the annual flooding of the lake occurs during the dry season (November to May) because of the time it takes for the water to travel through the Chari-Logone system to reach the lake (Leblanc et al., 2011).

Using land surface temperature and radar data from satellites, Policelli et al. [2018a] described the total lake area for the dry seasons of 1988–1989 through 2016–2017 as highly variable with a trend line increasing at about 140 km^2/year. Others, particularly at international conferences and in media reports, insist that the lake continues to shrink and will ultimately disappear (Magrin, 2016). This concern over a potentially disappearing Lake Chad has sparked numerous concepts centered on transferring water from the Congo River Basin to Lake Chad. This is also what has motivated our interest in building a statistical model of Lake Chad and forcing it with climate predictions. Our goal in this paper is to present the results of a statistical model for the area of Lake Chad built from a regression of precipitation, evapotranspiration (ET), and lake area data and forced with bias corrected precipitation and ET results from Global Climate Model simulations performed for the Coupled Model Intercomparison Project 5 (CMIP5, Taylor et al., 2011), established by the Working Group on Coupled Modeling under the World Climate Research Programme. In particular, we used the results from the CMIP5 model runs based on the Representative Concentration Pathway 8.5 (RCP 8.5). RCP 8.5 represents the highest greenhouse gas emissions scenario used in the CMIP5 models and includes high population growth, limited

technological change, and a radiative forcing that reaches 8.5 W m^{-2} by the end of the century. RCP 8.5 is considered a "baseline" scenario in which no climate mitigation policy is enacted (Riahi et al., 2011, Vuuren et al., 2011).

To the best of our knowledge, we produce here the first set of annual time series of projected Lake Chad area for the twenty-first century.

3.2 Data and Models

The data sets used in this study were: (1) Climate Hazards Group InfraRed Precipitation with Station data (CHIRPS, Funk et al., 2015), (2) ET data from the Famine Early Warning Systems Network (FEWS NET) Land Data Assimilation System (FLDAS, McNally et al., 2017) (3) the HydroSHEDS project's ("HydroSHEDS,", http://www.hydrosheds.org, Lehner et al., 2008) shape file for the southern Lake Chad Basin extent (4) Lake Chad total surface water area data from the research for Policelli et al. [2018a], (5) CMIP5 RCP 8.5 model results from the Koninklijk Nederlands Meteorologisch Instituut (KNMI) Climate Explorer ("Climate Explorer", https://climexp.knmi.nl/start.cgi), and (6) precipitation and ET data from the Global Land Data Assimilation System 2 (GLDAS2, Rodell et al., 2004).

The CHIRPS precipitation data is produced by the Climate Hazards Group at the University of California, Santa Barbara using both rain gauge data and satellite data. We used the daily Africa rainfall dataset, version 2, which has a resolution of .05 degree x .05 degree. The data is available from January, 1981 and is updated monthly. We used CHIRPS data from 1993 through 2016 to be consistent with the ET and lake area products. For Africa, CHIRPS has a mean bias of .22 for the wet season and a mean error of 79 mm per 3 months during the wet season (Funk et al., 2015). The bias is calculated as the absolute value of 1-mean (CHIRPS)/mean (GPCC) where GPCC refers to the precipitation estimates provided by the Global Precipitation Climatology Center. The error is relative to the GPCC dataset (Becker et al., 2013).

The FLDAS ET product is based on total ET from the Noah 3.3 Land Surface Model, and includes evaporation and transpiration from the canopy as well as evaporation from bare soil. The FLDAS ET product is available for October 1992 to the present. Evaluation of the FLDAS ET using the Simplified Surface Energy Balance model (Senay et al., 2013) indicates a limited ($r< 0.5$) but not insignificant correlation for West Africa percent ET variations (McNally et al., 2017).

The HydroSHEDS shape file for the southern Lake Chad Basin was provided by the World Wildlife Foundation (WWF). The shape file was used to calculate rainfall and ET for the hydrologically active portion of the basin. The HydroSHEDS database of basin shapes was developed by WWF using data from the NASA Shuttle Radar Topography Mission (SRTM).

Dry season total surface water area estimates for Lake Chad are from the research for Policelli et al. [2018a]. These were derived from (1) Land Surface Temperature (LST) data at 1 km resolution from the MODIS sensor on the NASA Terra satellite, and adjusted using Sentinel-1a C-band radar data from the European Space Agency, and (2) bias corrected total surface water area estimates of Lake Chad by (Leblanc et al., 2011) derived from Meteosat MVIRI sensor LST data at 5 km resolution. During the period of overlap, the estimated lake areas for (1) and (2) were within roughly 3% of each other. Because the lake (including flooded vegetation) is cooler than its surroundings during the day, LST data can be used to discriminate inundated areas from land (Leblanc et al., 2011). Total surface water area estimates of Lake Chad from the 1993 through the 2016 dry seasons were used in this research.

Through their Climate Explorer, KNMI provided precipitation and ET results from thirty-seven independent GCM's, eleven of which consisted of varying numbers of ensemble members, for a total of seventy-four CMIP5 RCP 8.5 simulations. We further generated

results for the ensembles by averaging the statistical model area results for each of the eleven CMIP5 RCP 8.5 models for which multiple realizations were available in the KNMI archive.

The GLDAS2 precipitation and ET data used is 0.25 degree resolution, monthly data for 1950-1989, derived from the Noah Model 3.3 Land Surface Model, forced by precipitation data from the Global Meteorological Forcing Dataset for land surface modeling from Princeton University (Sheffield et al., 2006). The Princeton University precipitation data blends observations with reanalysis data and disaggregates the data in space and time.

3.3 Methods

We developed our statistical model for the area of Lake Chad for the dry season months based on linear first order regression of the previous wet season's precipitation and ET, the previous year's area for the given month, and each month's area for the period of observations (1993-2016). For projected precipitation and ET, we used the RCP 8.5 climate simulations available through the web application, KNMI Climate Explorer. We used the seventy-four CMIP5 RCP 8.5 simulations available on Climate Explorer (including all ensemble members) to provide precipitation and ET from 1993 through 2100. In order to maintain continuity between the observed precipitation and ET and the simulated precipitation and ET, we bias corrected the CMIP5 RCP 8.5 simulation results for the period of observations and extended that correction for the projections. Having the statistical model for the lake area and bias corrected, modeled precipitation and ET for 1993-2100, we ran the seventy-four CMIP5 CRP 8.5 simulation results through this statistical model and averaged the monthly dry season lake area results. The statistical model was initialized with observed Lake Chad area and the model kept track of the previous year's area from each year's results. We allowed seven years for the statistical model to stabilize and only used the results from 2000-2100. We then generated an additional eleven simulations by averaging the area results from the models that were provided as a set of ensemble members, for a total of eighty-five

climate simulations.

The 85 CMIP5 RCP 8.5 simulations in combination with our statistical model provided a wide range of projected area for Lake Chad (see Section 4). In order to narrow this down, we evaluated projections for two subsets of the CMIP5 simulations: one consisting of the models that reproduced realistic statistics of lake area variability during the period of observations, and a second based on a previously published analysis of CMIP5 model performance in the Lake Chad headwaters region. Results of these model subsets are presented in Section 4.

3.3.1 Statistical models of lake area

The following equations for Lake Chad area during the dry season were arrived at through regression using methods described in Policelli et al [2018b]:

Eqn. 1: Area (November) = 10.43 x P-8.52 x ET+.76 x Last Year's Area (Nov.) -783

Eqn. 2: Area (December) = 13.35 x P-9.07 x ET+.78 x Last Year's Area (Dec.) -2803

Eqn. 3: Area (January) = 13.26 x P-3.85 x ET+.70 x Last Year's Area (Jan.) -3922

Eqn. 4: Area (February) = 18.96 x P-8.33 x ET+.70 x Last Year's Area (Feb.) -5811

Eqn. 5: Area (March) = 19.11 x P-5.26 x ET+.57 x Last Year's Area (March) -5684

Eqn. 6: Area (April) = 17.81 x P-2.12 x ET+.50 x Last Year's Area (April) -5402

Eqn. 7: Area (May) = 20.80 x P-0.17 x ET+.41 x Last Year's Area (May) -7629

P in these equations represents the past wet season's total precipitation. Similarly, ET represents the past wet season's total ET. We bias corrected the CMIP5 RCP 8.5 simulated precipitation and ET using CHIRPS precipitation data and FLDAS ET data, initialized "Last Year's Area" with observations, and then ran the equations for 1993-2100 using these data and keeping track of "Last Year's Area" for use in the equations. The specific regression equations used here differ from Policelli et al. [2018b] because in this study we are limited to

variables that can be derived from CMIP5 output; the previous study also made use of satellite altimetry and other parameters not available for these models.

We ran several tests on these equations to make sure that they were stable with regard to errors in "Last Year's Area". We initialized "Last Year's Area" with very high values then very low values to make sure that the equations would converge on the observed values. In both cases the results quickly converged. When we initialized the model with the previous year's area equal to the highest observed area, the average modeled dry season area returned to within ten percent of its observed value within five years (see figure 3.2, left). When we initialized the model with the previous year's area at 4000 km, (considerably lower than any of the observed or modeled values in this study) the average dry season area returned to within ten percent of its observed value within three years (see figure 3.2, right).

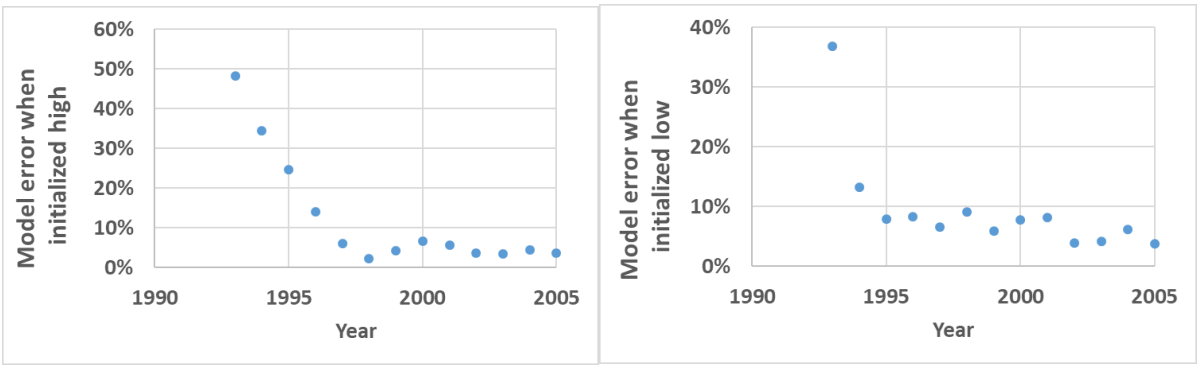

Fig. 3.2 When initialized with a very high value (left) or a very low value (right) the statistical model returns rapidly to within ten percent of the Lake Chad observed average dry season area

According to (Lemoalle, 2004), Lake Chad experienced a wet period from 1950 to 1971 and a dry period from 1972 to 1989 and the lake area decreased substantially due to this change. To get a sense of the ability of the statistical model to capture the high areas of the 1950-1971 wet period and the low areas of the 1972-1989 dry period independently of the CMIP5 models, we used precipitation and ET data from the NASA GLDAS model to force the statistical model, and compared the results with the water balance model by (Lemoalle,

2004). After being initialized in 1950 at 21,100 km^2, the average Lake Chad area for this configuration for the 1950-1971 wet period was 17,150 km^2 (Lemoalle's average was 21,100 km^2 for this period). For the 1972-1989 dry period, the average area for this configuration was 11,360 km^2 (Lemoalle's average for this period was 10,800 km^2). The GLDAS model results were used in this case because the GLDAS precipitation is more observation-based than that for the CMIP5 models. The GLDAS ET is modeled which may account for part of the discrepancy with Lemoalle's model. While we don't know at what area Lemoalle initialized his model, it would be necessary to initialize our statistical model at nearly 49,000 km^2 in order to average 21,100 km^2 for the wet period. This is highly unlikely, for either the actual lake, or Lemoalle's model.

During the period of observations (1993-2016), the wet season CHIRPS precipitation average was 752 km^3, the wet season FLDAS ET average was 499 km^3 and the lake area was between 8700 km^2 and 16,800 km^2. This data was used to train the statistical model. During 1950-1971, the GLDAS2 wet season precipitation averaged 808 km^3, the GLDAS2 wet season ET averaged 462 km^3, and our simulated lake area average was 17,150 km^2. The net precipitation and lake area for 1950-1971 as modeled by Lemoalle are clearly outside of the range of the training data. Assuming the GLDAS2 precipitation and ET and the Lemoalle model are all reasonably accurate, we conclude that our statistical model tends to underestimate the area of the lake for net precipitation and lake area greater than that used for the training period, but that the model does capture the general contrast between the high stand and low stand periods.

3.4 Results and Discussion

Running equations 1-7 using bias corrected P and ET from the full set of CMIP5 RCP 8.5 simulations and averaging the area over the dry seasons for 2000-2100 results in the range of projected area for Lake Chad shown in figure 3.3. The average for all of the simulations is

also shown in figure 3.3. The trend line of the average simulated dry season average area increased at a rate of approximately twenty-four km^2/year. The trend line of the standard deviation of the simulated dry season average areas increased at a rate of approximately forty-four km^2/year; this gives an indication of the increasing variability of the model results with increasing number of years the area is projected.

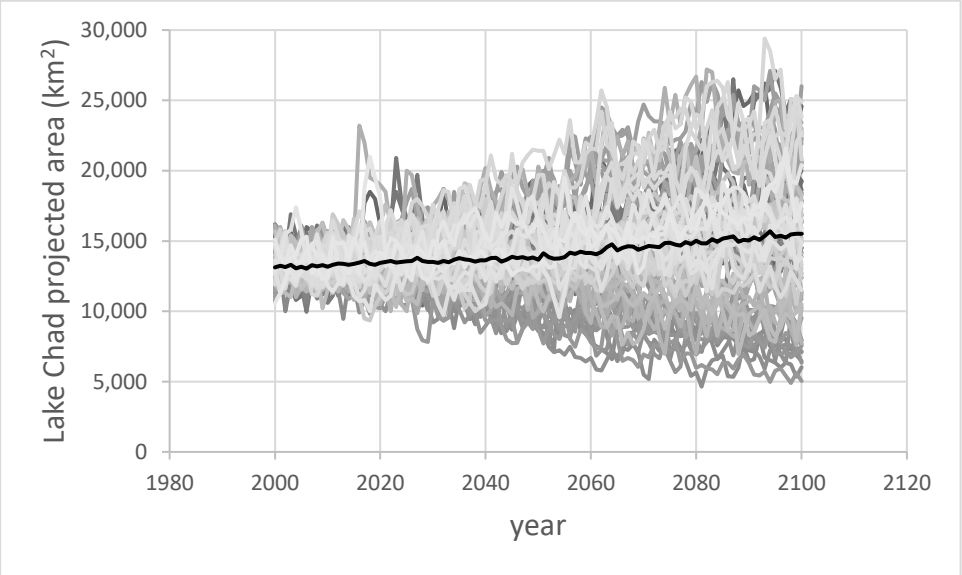

Fig.3.3 Lake Chad projected dry season average area from our statistical model driven by CMIP5 model results. Time series for eighty-five simulations are shown in grey; the average of all simulations is shown in black.

The average dry season lake area results from using all CMIP5 RCP 8.5 simulations for 2000-2016 averaged between 12,600 km^2 and 13,900 km^2, which is close to the average observed value for that period: 13,450 km^2. The interannual standard deviation in dry season average area, averaged across all simulations for 2000-2016 was 1100 km^2. In comparison, the interannual standard deviation in dry season average observed area for 2000-2016 was 1433 km^2. The ranges and standard deviations of lake area derived using CMIP5 RCP 8.5 output for the years 2021-2040, 2041-2060, 2061-2080, and 2081-2100 are shown in Table

3.1.

Table 3.1 Results from using all CMIP5 simulations for 20 year periods

	Min. of avg. dry season area averaged across indicated time span (km^2)	Max. of avg. dry season area averaged across indicated time span (km^2)	Interannual standard deviation in dry season average area, averaged across all simulations (km^2)
2021-2040	10,600	17,400	1200
2041-2060	8,900	20,800	1160
2061-2080	7,200	23,200	1190
2081-2100	5,800	24,400	1200

For 2021-2040, forty-eight of the eighty-five simulations project an increase in area relative to the average of observations for 2000-2016. For 2041-2060, fifty of the eighty-five simulations project an increase in area relative to the average for 2000-2016. For 2061-2080, sixty of the eighty-five simulations project an increase in area relative to the average for 2000-2016 and for 2081-2100 fifty-nine of the eighty-five simulations project an increase in area relative to the average for 2000-2016.

In order to down select appropriate models from the full set of CMIP5 RCP 8.5 models, we looked at the average and standard deviation for lake area from the models and compared these with the data during the period of observations. As mentioned above, the average of the models' Lake Chad average dry season area results during 2000-2016 matched well with the average of the observations for that period; the area from the models was in the range of roughly 6 percent less to 4 percent greater than the observations. This is likely due to the bias correction performed on the CMIP5 RCP 8.5 model data and the fact that the area observations were used in the regression to establish our statistical model. We found six CMIP5 RCP 8.5 models that additionally had standard deviations within plus or minus five percent of that for the observed area during 2000-2016. The six are: CanESM2, CCSM4, GISS-E2-R_p3, HadGEM2-ES, MRI-CGCM3 and NorESM1-ME. The results of using output from these models in the statistical model for Lake Chad area are shown in Fig. 3.4.

For the models that have ensemble members, we show the performance of the members in our statistical model as well as the average area derived from the members; as a consequence, 21 simulations are shown (plus the average of all the simulations).

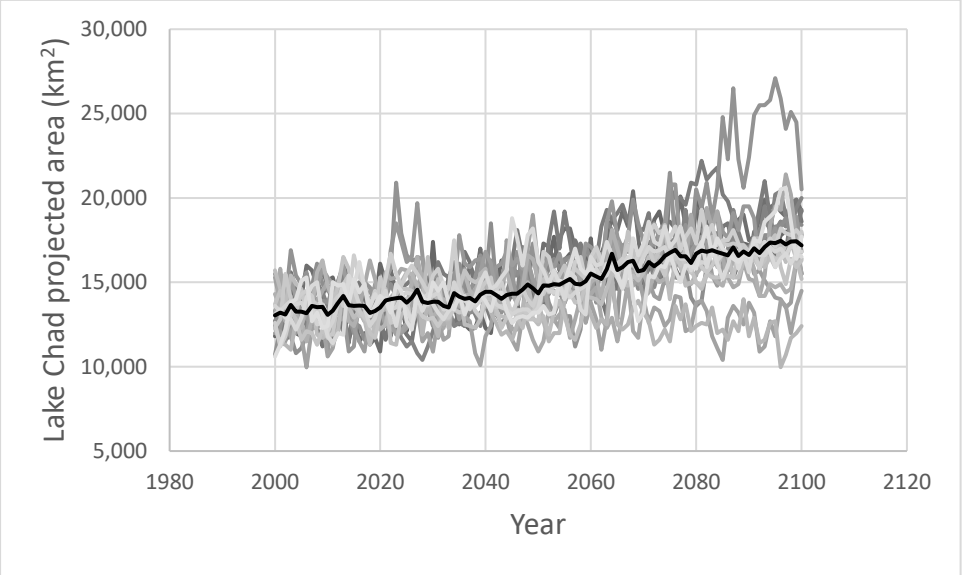

Fig. 3.4 Projected area of Lake Chad derived from 21 CMIP5 simulations which (in conjunction with the lake area statistical model) perform well modeling lake area during 2000-2016. The average performance of the 21 simulations is shown in black.

For these twenty-one simulations, the minimum average modeled dry season average Lake Chad area for 2000-2016 was 12,600 km^2 and the maximum average modeled dry season average area was 13,900 km^2. This again is close to the observed average value of dry season average area, which is 13,450 km^2. The rate of increase of the trend line of the average of the twenty-one simulations is forty-six km^2/year; this is significantly higher than the rate of increase of the trend line for the full set of eighty-five simulations. The interannual standard deviation in dry season average area, averaged across these simulations during 2000-2016 was 1160 km^2. The ranges and standard deviations of dry season average area for these models, when run in conjunction with our statistical model, for the average of years 2021-

2040, 2041-2060, 2061-2080, and 2081-2100 are shown in Table 3.2.

Table 3.2 Results derived from CMIP5 models which performed well in combination with the statistical model during the period of observations

	Min. of avg. dry season area averaged across indicated time span (km^2)	Max. of avg. dry season area averaged across indicated time span (km^2)	Interannual standard deviation in dry season average area, averaged across the 21simulations (km^2)
2021-2040	12,300	16,000	1060
2041-2060	13,000	15,900	1170
2061-2080	12,700	18,700	1160
2081-2100	12,100	23,400	1090

The results in Table 3.2 show a substantial decrease in the range of lake area projections relative to the results for all of the CMIP5 RPC 8.5 simulations shown in Table 3.1. For 2021-2040, seventeen of the twenty-one simulations project an increase in area relative to the average of observations for 2000-2016; for 2041-2060, eighteen simulations project an increase, for 2061-2080, twenty simulations project an increase, and for 2081-2100, nineteen simulations project an increase. Figure 3.5 shows the standard deviation for these CMIP5 RCP 8.5 simulation results when run in our statistical model. The trend line of the standard deviation of the model results increases at a rate of approximately fourteen km^2/year.

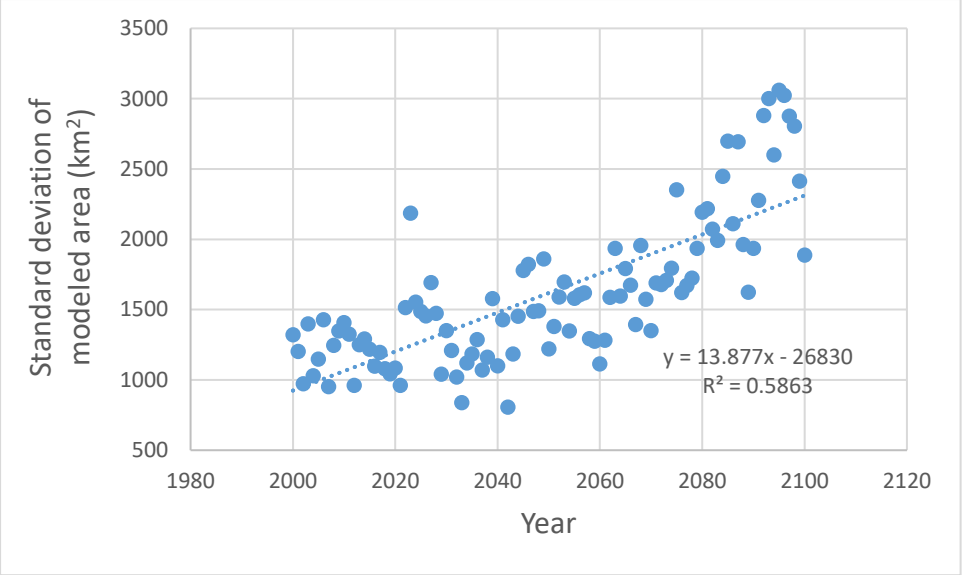

Fig. 3.5 Standard deviation for twenty-one selected CMIP5 simulations when run in conjunction with our statistical model. The twenty-one simulations were based on six models and were selected based on skill in modeling Lake Chad area during 2000-2016 when used with our statistical model.

An alternative set of CMIP5 RCP 8.5 models can be down-selected based on (Fotso-Nguemo Thierry C. et al., 2018) in which the researchers identified eleven GCM's run under the RCP 8.5 scenario for which the precipitation product performed well compared with observations in Central Africa. They define Central Africa as being between 15°S and 15°N latitude, and 5°E and 35°E longitude. This includes most of the Southern Lake Chad Basin. The catchments for the Chari and Logone Rivers, which, as already mentioned, provide ninety percent of the water flowing to Lake Chad (Zhu et al., 2017) are well within these boundaries. We were able to access the results from nine of these eleven "highly performing" models: ACCESS1–0, BNU-ESM, CanESM2, EC-EARTH, GFDL-CM3, HadGEM2-ES, MPI-ESM-LR, MPI-ESM-MR, and MRI-CGCM3. Note: CanESM2, HadGEM2-ES, and MRI-CGCM3 were included in both sets of down selected models.

Again, for the models that were provided as a set of ensemble members, we created an area average for the ensemble members when used with our statistical model to represent the

model. With the nine models and associated ensemble members, there were twenty-three simulations. When using the precipitation and ET results from these twenty-three simulations as input to our statistical model for Lake Chad area, we derived the following results (Fig. 3.6)

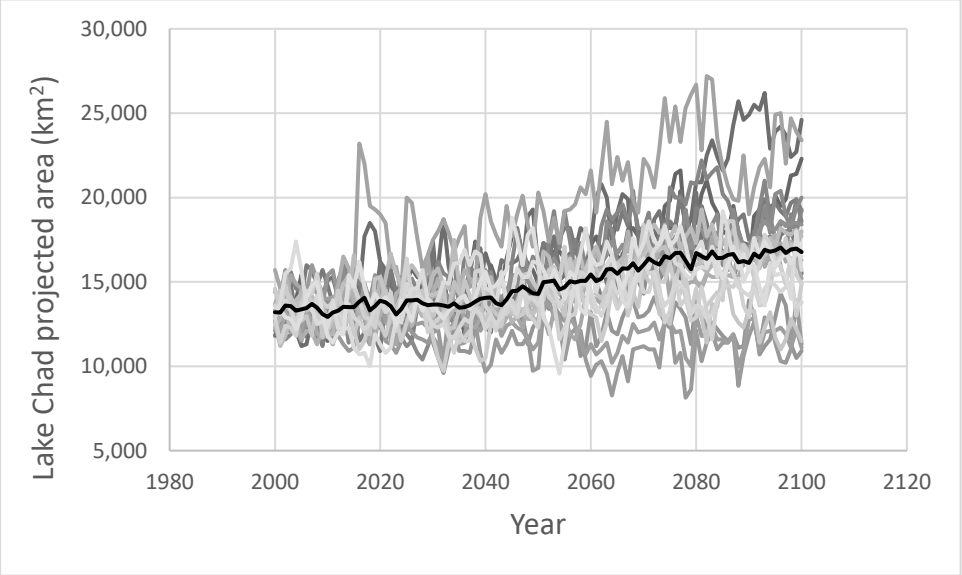

Fig. 3.6 Projected area of Lake Chad using 23 simulations from 9 CMIP5 models which perform well modeling precipitation in central Africa
(Fotso-Nguemo Thierry C. et al., 2018)

For these twenty-three simulations, the minimum modeled average dry season Lake Chad area for 2000-2016 was 12,700 km^2 and the maximum modeled area was 13,900 km^2. This is once again close to the observed value of 13,450 km^2. The rate of increase of the trend line of the average of the twenty-three simulations is 43 km^2/year; this is again significantly higher than the rate of increase of the trend line for the full set of eighty-five simulations. The interannual standard deviation in dry season average area, averaged across these simulations during the period of observations was 1140 km^2. The results of these simulations in combination with the statistical model for the average of years 2021-2040, 2041-2060, 2061-2080, and 2081-2100 are shown in Table 3.3. They represent a somewhat more narrow

range of results than the entire set of CMIP5 RCP 8.5 simulations (Table 3.1).

Table 3.3 Results derived from CMIP5 simulations for which precipitation performed well in central Africa (Fotso-Nguemo Thierry C. et al., 2018)

	Min. of avg. dry season area averaged across indicated time span (km^2)	Max. of avg. dry season area averaged across indicated time span (km^2)	Interannual standard deviation in dry season average area, averaged across the 23 simulations (km^2)
2021-2040	11,800	17,400	1090
2041-2060	11,500	18,900	1170
2061-2080	10,400	22,700	1140
2081-2100	11,400	23,700	1110

For 2021-2040, fourteen of the twenty-three simulations project an increase in area relative to the average of observations for 2000-2016; for 2041-2060, nineteen simulations project an increase, for 2061-2080, twenty simulations project an increase, and for 2081-2100, nineteen simulations project an increase. Fig. 3.7 shows the standard deviation for these simulations when run with our statistical model. The trend line of the standard deviation of the simulation results increases at a rate of approximately twenty-four km^2/year.

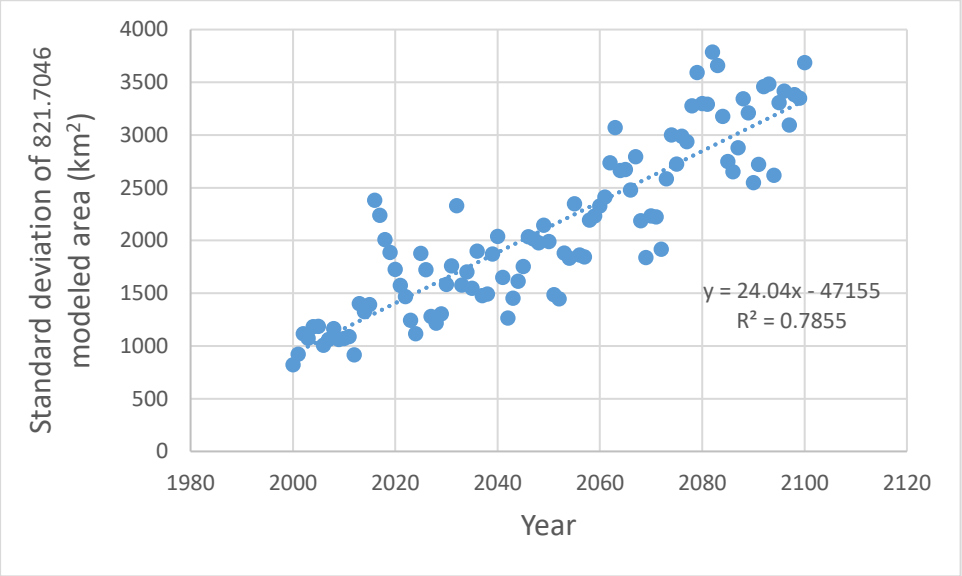

Fig. 3.7 standard deviation derived from 23 CMIP5 RCP 8.5 simulations which perform well modeling precipitation in West Africa (Fotso-Nguemo Thierry C. et al., 2018)

Precipitation in the region of Lake Chad is driven by the West African monsoon. Gaetani et al., 2017 argue that the spread in precipitation results among the CMIP5 models for this region is due to different model sensitivities to the competing influences of the direct and indirect effects of increased CO_2 . The direct effect of increased CO_2 includes warming of the Sahara, forcing an increased meridional energy gradient and strengthening the monsoonal circulation. The indirect effect of increased CO_2 is a general warming of sea surface temperatures causing a decrease in the regional meridional energy gradient and weakening of the monsoonal circulation (Gaetani et al., 2017).

When forced by the precipitation and ET output of the CMIP5 RCP 8.5 simulations and initialized at 21,100 km^2, the statistical model was not able to replicate the lake area of the wet period of 1950-1971 given by the water balance model by (Lemoalle, 2004). For this period, the average area from the CMIP5 RCP 8.5/statistical model system was 13,300 km^2 with a standard deviation of 1187 km^2 (Lemoalle's model averaged 21,100 km^2 for this period). The CMIP5 RCP 8.5 meteorological fields yielded area estimates that were closer to those modeled by Lemoalle in the dry period of 1972-1989. The average lake area from the CMIP5 RCP 8.5/statistical model system for the dry period was 12,000 km^2 with a standard deviation of 1631 km^2 (Lemoalle's average for this period was 10,800 km^2). Nine of the CMIP5 RCP 8.5 simulations coupled with the statistical model produced lake areas of 10,800 +/- 200 km^2. The absence of a clear wet to dry transition in the historical CMIP5 models is unsurprising, since these are coupled models that are not expected to capture internal climate variability. The result, therefore, is consistent with the understanding that the reduction in Lake Chad's area between the 1950-1971 and 1972-1989 periods is a result of natural climate variability and/or increased water withdrawals due to direct human activity or ecological change. It is also possible that the shift is part of a longer term trend in which the Lake is still shrinking in response to climatic or environmental change in the more distant past, and that

lake area is simply not in equilibrium with the basin's water balance. Recent increases in lake area, however, suggest that lake area patterns are not the product of adjustment in response to long-term historical disequilibrium.

3.5 Conclusions

We examined the results of running a statistical model of the dry season area of Lake Chad forced by bias corrected precipitation and evapotranspiration from CMIP5 RCP 8.5 simulations for the years 2000-2100. The model performed well for the period of observations. The spread of projected model results was fairly broad, for instance ranging from an average of 5,800 km^2 to an average of 24,400 km^2 for the years 2081-2100. However, there was no scenario under which our modeled lake "disappeared" as expected by some (Magrin, 2016). In fact, for the years 2081-2100, fifty-nine of the eighty-five simulations tested projected an increase in area during the dry season relative to the average of the observations for 2000-2016. The trend line for the average of all simulations shows a rate of increase of approximately twenty-four km^2/year (approximately 0.2 percent of the observed lake area for 2000-2016 per year).

We used two different methods to down-select CMIP5 RCP 8.5 models that we expected to best represent the climate of the Lake Chad catchment. For the first method, we selected six models (for which we had a total of twenty-one simulations) that had the best results compared to observations of the variability of Lake Chad area for 2000-2016 when used to force the statistical model. We used standard deviation as the measure of variability during 2000-2016 to select the best models. Because the models' average areas were all close to the observed, we did not use average area to down select models. The average rate of increase of Lake Chad area for 2000-2100 based on these simulations was approximately forty-six km^2/year (approximately 0.3 percent of the observed lake area for 2000-2016 per year).

For the second method, we chose nine CMIP5 models, (for which we had a total of

twenty-three simulations) this time based on the performance of precipitation in West Africa as described in (Fotso-Nguemo Thierry C. et al., 2018). The average rate of increase of Lake Chad area for 2000-2100 based on these simulations was forty-three km^2/year (approximately 0.3 percent of the observed lake area for 2000-2016 per year).

A caveat to understanding the results presented here is that there is increased uncertainty in the CMIP5 RCP 8.5/statistical model results when the results are greater or less than the range of areas used during the training of the statistical model. Another consideration is that the measurement and projections presented here are for the Lake Chad dry season; the lake reaches its minimum annual elevation in June, during the wet season (Policelli et al., 2018b). There is also the strong possibility that Lake Chad will respond during the projected period to forcing by internal climate variability not fully accounted for in the CMIP5 models, such as caused by the El Nino/La Nina Southern Oscillation, the Atlantic Multidecadal Oscillation and combinations of these phenomena (Okonkwo et al., 2015), and widespread biomass burning across Africa (Ichoku et al., 2016). Possible future anthropogenic changes in the hydrologic system of the Lake Chad basin, such as large irrigation projects, or the proposed diversion of water from the Congo Basin to Lake Chad, are also not accounted for in our model. More precise projections of the area of Lake Chad using the method developed here also depend on better and more consistent projections of the precipitation and ET in the Lake Chad catchment caused by climate change. This will likely involve better modeling of the sensitivity of the West African Monsoon to the competing impacts of generally increased sea surface temperatures and greater heating of the Sahara (Gaetani et al., 2017). Additionally, improvements to the models and satellite data retrievals for the data types used to develop and initialize the regression model will likely have a significant beneficial effect on the projections. Future attempts to project the area of Lake Chad should also consider using a suitable physically-based model of the lake and catchment in place of the statistical model

used here. Finally, it is possible that the world will follow a different Representative Concentration Pathway than the "baseline" RPC 8.5 models used in this study, in which case the projected area of Lake Chad could be quite different.

Conclusion

The subject of this dissertation is the area of Lake Chad, including its recent fluctuations, near term forecasting of its dry season area, and projections of its dry season area for the 21st century. The inspiration for writing this dissertation has been the fact that there is a great deal of disagreement in the scientific literature and the popular press about the recent history of Lake Chad's surface water area and of the fate of the lake in the coming years. Given the multitude of imaging satellites providing data, much of it free to the public, the recent area of the lake would seem to be an easy problem to solve. However, most of the lake in its current state is covered with aquatic vegetation, and use of data from widely used optical imaging systems cannot readily detect and measure this contribution to the lake's area. As a consequence, it seems that many of the would-be chroniclers of the lake's area are only including the open water area and are highly underestimating the total lake area (e.g. Birkett, 2000).

In our first paper, "Lake Chad Total Surface Water Area as Derived from Land Surface Temperature and Radar Remote Sensing Data" we took on the challenge of measuring the dry season area of Lake Chad for the late twentieth century and early twenty-first century (1988-2017). The key to measuring the total water of the lake (open water and flooded vegetation) was use of Land Surface Temperature (LST) data derived from thermal infrared satellite measurements, and use of radar imaging data. LST data indicates lower temperatures during the day for open water and flooded vegetation, (Leblanc et al., 2011) and the contrast between bare ground and dry vegetation on the one hand and open water and flooded vegetation on the other is especially sharp during the dry season in the arid environment of Lake Chad. Our focus on measuring the lake area during the dry season (November through May) stems from the fact that the LST data does not distinguish well between wet soil and flooded vegetation. Because of the great distance from the headwaters of the main tributaries

(the Chari and Logone Rivers) to the lake, the dry season is also the time when the lake experiences its annual flood pulse. We used LST data from the MODIS sensor on the NASA Terra satellite, which was available for the dry seasons of 2000-2001 through 2016-2017. However, based on a review of the literature, including (White et al., 2015, Henderson and Lewis, 2008, Guo et al., 2017) we considered radar to be the best data source to use for measuring the total lake area. Unfortunately, most unclassified radar data are collected by commercial or quasi-commercial entities and are not readily available to the scientific community. This changed with the free and open distribution of C-band radar data from the European Space Agency's Sentinel-1a satellite, which began collecting data in April 2015. To take advantage of the expected higher performance of the radar data and the longer record of the LST data, we used the radar data to bias correct the areas corresponding to the three main divisions of Lake Chad: the "southern pool", the "northern pool", and the "archipelago". In addition to the bias corrected MODIS LST data, we had available to us estimates of Lake Chad area using LST data from the EUMETSAT Meteosat satellite MVIRI sensor for 1988-2001 by (Leblanc et al., 2011). When we compared our bias corrected area estimates with the areas estimated by Leblanc during the period of overlap, we found a relatively close match; our estimates were approximately three percent higher than Leblanc's. Combining our estimates with Leblanc's estimates, we had a time series of Lake Chad area for the 1988-1989 dry season through the 2016-2017 dry season. The data is plotted in Figure 1.8 of the first paper and shows a highly variable area with a trend line increasing at approximately 143 km^2/year. For the period of observations, the maximum total surface water area of the lake was approximately 16,800 km^2, the minimum total surface water area of the lake was approximately 6,400 km^2, and the average was approximately 12,700 km^2.

In our second paper, "A predictive model for Lake Chad total surface water area using remotely sensed and modeled hydrological and meteorological parameters and multivariate

regression analysis", we used linear first order regression to develop a statistical model consisting of a set of equations for predicting the monthly average lake area for the next dry season (excluding November). Because only the southern part of the Lake Chad Basin is hydrologically active (generates runoff that reaches the lake), we limited our analysis to that part of the basin. We used the estimated lake area data from the first paper as the dependent variable in the regression analysis to train the model, and we used wet season precipitation and evapotranspiration, lake evapotranspiration as a percentage of the 1988-2016 average, November lake elevation variation relative to the 2002-2009 average, and the previous year's lake area for the given month as the independent variables. We used backward elimination to limit the number of variables in the equations to the ones that mattered most. This involved fitting all of the variables into the model, then removing the variable with the highest p-value and re-running the regression; this was repeated so that we were left with three independent variables. We limited the equations to three independent variables to limit the risks of overfitting the data. To estimate the error of the equations, we conducted a Leave One Out Cross Validation (LOOCV) analysis. This involved removing one data point from the training data, calculating the regression equation, evaluating the error for the removed data point, returning the data point to the dataset, and repeating the process until each data point had been removed and evaluated, and then averaging the error values generated in this way. Using the LOOCV analysis, we estimated that the average absolute error ranged from 5.3 percent (for February estimates) to 7.6 percent (for May estimates). These errors were well below the errors estimated for either using the previous year's area for a given month as the estimate for the current year, or for using the historical average area for a given month as the estimate for the current year.

In our third paper, "Projections of Lake Chad total surface water area derived by forcing a statistical model of the lake area with results of climate simulations through the year 2100"

we developed a first order linear regression for the lake area using only the wet season precipitation and evapotranspiration for the southern Lake Chad Basin, and the lake area for the given month of the previous year. These are variables that can be obtained from climate models or calculated internally to the model. We worked with eighty-five Coupled Model Intercomparison Project 5 (CMIP5) Representative Concentration Pathway (RCP) 8.5 climate simulations, including seventy-four model variations and ensemble members available through the KNMI Climate Explorer ("Climate Explorer", https://climexp.knmi.nl/start.cgi.), and eleven ensemble derived averages. The precipitation and evapotranspiration from the climate simulations were bias corrected using the training data for the statistical model. The statistical model was initialized with observed lake area for the first year and the model kept track of the previous year's area for use in the calculation of the next year's lake area. We did not use the results for 1993-1999 to allow for model spin up. The result was eighty-five time series of projected lake area for the dry seasons of 2000-2100. The trend line of the average of the eighty-five simulations increased at a rate of approximately twenty-four km^2/year. The annual average dry season lake area for the eighty-five simulations did not drop below 4,500 km^2. The projections for the dry season average lake area averaged over the years 2081-2100 ranged from 5,800 km^2 to 24,400 km^2. We developed two methods to down select sets of models that were expected to perform the best. For the first method, we selected the models that performed the best during 2000-2016 (during the period of observations). Because all of the simulations performed well estimating the area of the lake during 2000-2016, we chose standard deviation as a measure of variability to be our figure of merit. This resulted in the selection of twenty-one simulations representing six models. The trend line for the average of these simulations increased at a rate of approximately forty-six km^2/year, nearly double that for the full set of eighty-five simulations. The annual average dry season lake area for the twenty-one simulations did not drop below 9,900 km^2. The

projections for the dry season average lake area averaged over the years 2081-2100 ranged from 12,100 km^2 to 23,400 km^2, a significant decrease in the projected range of the area for those years compared with the projections for the full set of eighty-five simulations. For the second method, we selected the twenty-three simulations from nine models that perform well modeling precipitation in central Africa according to (Fotso-Nguemo Thierry C. et al., 2018). The trend line for the average of these simulations increased at a rate of approximately forty-three km^2/year, considerably higher than that for the full set of eighty-five simulations. The annual average dry season lake area for the twenty-one simulations did not drop below 8,100 km^2. The projections for the dry season average lake area averaged over the years 2081-2100 ranged from 11,400 km^2 to 23,700 km^2, again a significant decrease in the projected range of the area for those years compared with the projections for the full set of eighty-five simulations. There were three models which were included in the selection from both methods.

There are a number of limitations to the research presented here that must be considered. For instance, we were not able to measure the total lake area during the wet season for reasons described above. If we were able to do so, we would find that the minimum annual lake area occurs during the wet season (figure 2.6.b. in the second chapter shows that on average, the lowest lake surface elevation occurs in June, during the wet season). Additionally, the method of determining total lake area during the dry season has uncertainty that we cannot quantify; for instance, evaporative cooling of well-watered vegetation without standing water could decrease the LST for certain areas enough to erroneously group the area with the flooded vegetation, though this is likely a relatively small area given that we are doing the measurements during the dry season in the arid environment of Lake Chad. For the statistical modeling of Lake Chad area, there is uncertainty in each of the data sets used to train the models, and there is the caveat that the model performance is likely degraded for

areas greater or less than that of the training data. There is also inherent uncertainty in the statistical models of lake area because they do not represent the hydrological processes occurring in nature. Finally, in the third paper we limited our use of CMIP5 climate models to those using the "baseline" RCP 8.5 scenario (Riahi et al., 2011, Vuuren et al., 2011). If the world goes down a different carbon pathway, the results of the Lake Chad area projections could be quite different.

The results of this dissertation are significant in that (1) they provide an updated time series of estimated total Lake Chad area and trend using methods designed to include both flooded vegetation and open water, (2) a method was developed to estimate the average lake area for the months of December through May during which the annual flood often impacts the livelihoods of farmers along the borders of Lake Chad, and (3) a similar method was developed to project the total area of Lake Chad for the dry seasons through the end of this century. This last item has the potential to be used to inform the on-going discussion over whether to divert water from the Congo Basin to Lake Chad, a project with an estimated cost of $14.5 billion, and likely unforeseeable ecological impacts.

Future research is needed to address the limitations of this research as indicated above. For instance: (1) the use of radar data for estimating the Lake Chad wet season total area might be feasible. If an adequate database of radar acquisitions of the lake during the wet season and/or the dry season could be built up, a useful time series of lake total area might be developed, (2) if improved data sets for our independent variables in the regression analysis become available, it would be useful to repeat the modeling of the lake area, (3) the data from the climate simulations could potentially be used to force an appropriate physical model of the lake; it would be interesting to compare results between our statistical model and a physical model, and (4) the statistical modeling of the area of Lake Chad could be repeated

using data from other CMIP5 RCP scenarios, or using data from CMIP6 when it becomes available.

Appendix

We examined the correlation between P–ET for the southern Lake Chad Basin and the lake elevation variation relative to 1993-2002 for 1992 to 2017, and found the maximum correlation of 0.69 at four months lag time between these variables. Next, we examined the correlation between the P–ET for the southern part of the basin and the lake surface area and found the maximum correlation of 0.37 at eight months lag time. We also examined the correlation between the lake elevation variation and the lake surface water area and found the maximum correlation of 0.57 at four months lag time. We found a maximum correlation of 0.43 for ET vs the lake's surface water area at 7 months, and a correlation of 0.63 for the surface water area versus the previous year's surface water area for the same month. There is apparently memory of the previous year's area in the system.

To determine the value added by the ET data to our analysis, we examined the correlation between precipitation (without subtracting ET) for the southern Lake Chad Basin and the lake elevation and found an increase in the maximum correlation to 0.80 at four months lag time. We found the correlation between the percentage of the 1988-2016 average lake ET and the lake total surface water area to be 0.65 at zero lag time. We also examined the correlation between precipitation and total lake surface area and found an increase in the maximum correlation to 0.39 at seven months lag time. This is the same lag time as for the maximum correlation between ET and total lake surface area and represents the time it takes for much of the net precipitation to make its way from run off in the southernmost part of the Lake Chad basin, to flowing through the Chari-Logone River system, to reaching the lake and causing an increase in the lake area. A surprising result of the correlation analysis is that the use of FLDAS ET data in the analysis to produce (P-ET) causes a small decrease in the correlation numbers relative to what is achieved with precipitation alone. Note however that ET is somewhat more closely correlated with total lake surface water area than is

precipitation (.43 vs. .39, both at 7 months lag time). Precipitation and ET have a maximum correlation coefficient of 0.93 with a one month delay between the two.

Bibliography

Austin, P.C., Steyerberg, E.W., 2015. The number of subjects per variable required in linear regression analyses. J. Clin. Epidemiol. 68, 627–636. https://doi.org/10.1016/j.jclinepi.2014.12.014

Bader, J.-C., Lemoalle, J., Leblanc, M., 2011. Modèle hydrologique du lac Tchad. Hydrol. Sci. Journal–Journal Sci. Hydrol. 56, 411–425.

Badr, H.S., Dezfuli, A.K., Zaitchik, B.F., Peters-Lidard, C.D., 2016. Regionalizing Africa: Patterns of Precipitation Variability in Observations and Global Climate Models. J. Clim. 29, 9027–9043. https://doi.org/10.1175/JCLI-D-16-0182.1

Becker, A., Finger, P., Meyer-Christoffer, A., Rudolf, B., Schamm, K., Schneider, U., Ziese, M., 2013. A description of the global land-surface precipitation data products of the Global Precipitation Climatology Centre with sample applications including centennial (trend) analysis from 1901–present. Earth Syst. Sci. Data 5, 71–99. https://doi.org/10.5194/essd-5-71-2013

Biasutti, M.; Giannini, A., 2006. Robust Sahel drying in response to late 20th century forcings. *Geophys. Res. Lett. 33*.

Birkett, C.M., 2000. Synergistic remote sensing of Lake Chad: Variability of basin inundation. Remote Sens. Environ. 72, 218–236.

Bouchez, C.; Goncalves, J.; Deschamps, P.; Vallet-Coulomb, C.; Hamelin, B.; Doumnang, J.-C.; Sylvestre, F. Hydrological, chemical, and isotopic budgets of Lake Chad: A quantitative assessment of evaporation, transpiration and infiltration fluxes. *Hydrol. Earth Syst. Sci.* **2016**, *20*, 1599–1619.

Bowling, L.C.; Lettenmaier, D.P., 2009. Modeling the Effects of Lakes and Wetlands on the Water Balance of Arctic Environments. *J. Hydrometeorol. 11*, 276–295.

Broxton, P.D.; Zeng, X.; Sulla-Menashe, D.; Troch, P.A., 2014. A global land cover climatology using MODIS data. *J. Appl. Meteorol. Climatol. 53*, 1593–1605.

Busker, T., de Roo, A., Gelati, E., Schwatke, C., Adamovic, M., Bisselink, B., Pekel, J.-F., Cottam, A., 2018. A global lake and reservoir volume analysis using a surface water dataset and satellite altimetry. Hydrol. Earth Syst. Sci. Discuss. 1–32. https://doi.org/10.5194/hess-2018-21

Carmouze, J.-P., Durant, J.R., Lévêque, C., 1983. Lake Chad: ecology and productivity of a shallow tropical ecosystem. Springer Science & Business Media: Dordrecht, The Netherlands, Volume 53.

Characteristics of Lake Chad Level Variability and Links to ENSO, Precipitation, and River Discharge. Available online: https://www.researchgate.net/publication/269573424_Characteristics_of_Lake_Chad_Level_Variability_and_Links_to_ENSO_Precipitation_and_River_Discharge (accessed on 29 January 2018).

Climate Explorer: About the Climate Explorer [WWW Document], n.d. URL https://climexp.knmi.nl/about.cgi?id=someone@somewhere (accessed 4.30.18).

Coe, M.T., Birkett, C.M., 2004. Calculation of river discharge and prediction of lake height from satellite radar altimetry: Example for the Lake Chad basin. Water Resour. Res. 40, W10205. https://doi.org/10.1029/2003WR002543

Coe, M.T., Foley, J.A., 2001. Human and natural impacts on the water resources of the Lake Chad basin. J. Geophys. Res. Atmospheres 106, 3349–3356. https://doi.org/10.1029/2000JD900587

Delclaux, F., Le Coz, M., Coe, M., Favreau, G., Ngounou Gatcha, B., 2008. Confronting models with observations for evaluating hydrological change in the lake chad basin, Africa, in: XIIIth World Water Congress. URL: https://www.iwra.org/member/congress/resource/abs355_article.pdf accessed 7/18/2018

Fotso-Nguemo Thierry C., Chamani Roméo, Yepdo Zéphirin D., Sonkoué Denis, Matsaguim Cédric N., Vondou Derbetini A., Tanessong Roméo S., 2018. Projected trends of extreme rainfall events from CMIP5 models over Central Africa. Atmospheric Science Letters 19, e803. https://doi.org/10.1002/asl.803

Funk, C., Peterson, P., Landsfeld, M., Pedreros, D., Verdin, J., Shukla, S., Husak, G., Rowland, J., Harrison, L., Hoell, A., Michaelsen, J., 2015. The climate hazards infrared precipitation with stations—a new environmental record for monitoring extremes. Sci. Data 2, sdata201566. https://doi.org/10.1038/sdata.2015.66

Gaetani, M., Flamant, C., Bastin, S., Janicot, S., Lavaysse, C., Hourdin, F., Braconnot, P., Bony, S., 2017. West African monsoon dynamics and precipitation: the competition between global SST warming and CO<Subscript>2</Subscript> increase in CMIP5 idealized simulations. Clim. Dyn. 48, 1353–1373. https://doi.org/10.1007/s00382-016-3146-z

Gao, H., Bohn, T.J., Podest, E., McDonald, K.C., Lettenmaier, D.P., 2011. On the causes of the shrinking of Lake Chad. Environ. Res. Lett. 6, 034021.

Grove, A.T., 1996. African river discharges and lake levels in the twentieth century. Limnol. Climatol. Paleoclimatology East Afr. Lakes Gordon Breach Neth. 95–100.

Grove, A.T., 2008. A brief consideration of climate forcing factors in view of the Holocene glacier record. Global and Planetary Change, Historical and Holocene glacier – climate variations 60, 141–147. https://doi.org/10.1016/j.gloplacha.2006.07.033

Guo, M., Li, J., Sheng, C., Xu, J., Wu, L., 2017. A Review of Wetland Remote Sensing. Sensors (Basel) 17. https://doi.org/10.3390/s17040777

Harrell, F.E., Lee, K.L., Mark, D.B., 1996 Multivariable Prognostic Models: Issues in Developing Models, Evaluating Assumptions and Adequacy, and Measuring and

Reducing Errors. Stat. Med. 15, 361–387. https://doi.org/10.1002/(SICI)1097-0258(19960229)15:4<361::AID-SIM168>3.0.CO;2-4

Henderson, F.M., Lewis, A.J., 2008. Radar Detection of Wetland Ecosystems: A Review. Int.

J. Remote Sens. 29, 5809–5835. https://doi.org/10.1080/01431160801958405

Hess, L.L.; Melack, J.M.; Novo, E.M.L.M.; Barbosa, C.C.F.; Gastil, M., 2003. Dual-season mapping of wetland inundation and vegetation for the central Amazon basin. *Remote Sens. Environ. 87*, 404–428.

HydroSHEDS [WWW Document], n.d. URL http://www.hydrosheds.org/ (accessed 10.16.17).

Ichoku, C., L. T. Ellison, K. E. Willmot, et al. 2016. "Biomass burning, land-cover change, and the hydrological cycle in Northern sub-Saharan Africa." *Environmental Research Letters*, **11 (9):** 095005 [10.1088/1748-9326/11/9/095005]

Inter-basin water transfer: Opportunities, prospects for Lake Chad https://www.environewsnigeria.com/inter-basin-water-transfer-opportunities-prospects-lake-chad/, 2018, accessed 11/14/2018

Islam, T.; Hulley, G.C.; Malakar, N.K.; Radocinski, R.G.; Guillevic, P.C.; Hook, S.J., 2017 A Physics-Based Algorithm for the Simultaneous Retrieval of Land Surface Temperature and Emissivity From VIIRS Thermal Infrared Data. *IEEE Trans. Geosci. Remote Sens. 55*, 563–576

Jones, H.G.; Rotenberg, E.; Jones, H.G.; Rotenberg, E., 2011. Energy, Radiation and Temperature Regulation in Plants. In *eLS*; John Wiley & Sons: New York, NY, USA.

Jung, H.C.; Alsdorf, D., 2010. Repeat-pass multi-temporal interferometric SAR coherence variations with Amazon floodplain and lake habitats. *Int. J. Remote Sens. 31*, 881–901.

Kasischke, E.S.; Tanase, M.A.; Bourgeau-Chavez, L.L.; Borr, M., 2011. Soil moisture limitations on monitoring boreal forest regrowth using spaceborne L-band SAR data. *Remote Sens. Environ. 115*, 227–232.

Lake Chad flooded savanna", World Wildlife Fund, no date, https://www.worldwildlife.org/ecoregions/at0904 accessed 7/18/2018

Lake Chad|World Lake Database-ILEC. Available online: http://wldb.ilec.or.jp/Details/lake/AFR-02 (accessed on 20 July 2017).

Leblanc, M., Lemoalle, J., Bader, J.-C., Tweed, S., Mofor, L., 2011. Thermal remote sensing of water under flooded vegetation: New observations of inundation patterns for the 'Small' Lake Chad. J. Hydrol. 404, 87–98. https://doi.org/10.1016/j.jhydrol.2011.04.023

Lehner, B., Grill G., 2013. Global river hydrography and network routing: baseline data and new approaches to study the world's large river systems. Hydrological Processes, 27(15): 2171-2186.

Lehner, B., Verdin, K., Jarvis, A., 2011 New Global Hydrography Derived From Spaceborne Elevation Data. Eos Trans. Am. Geophys. Union 89, 93–94. https://doi.org/10.1029/2008EO100001

Lemoalle, J., 2004. Lake Chad: A Changing Environment. In: Nihoul J.C.J., Zavialov P.O., Micklin P.P. (eds) Dying and Dead Seas Climatic Versus Anthropic Causes. NATO Science Series: IV: Earth and Environmental Sciences, vol 36. pp. 321–339 Springer: Dordrecht, The Netherlands

Lemoalle, J., Bader, J.-C., Leblanc, M., Sedick, A., 2012. Recent changes in Lake Chad: Observations, simulations and management options (1973–2011). Glob. Planet. Change 80, 247–254.

Magrin, G., 2016. The disappearance of Lake Chad: history of a myth. J Polit Ecol 23, 204–222.

McNally, A., Arsenault, K., Kumar, S., Shukla, S., Peterson, P., Wang, S., Funk, C., Peters-Lidard, C.D., Verdin, J.P., 2017. A land data assimilation system for sub-Saharan Africa food and water security applications. Sci. Data 4, 170012. https://doi.org/10.1038/sdata.2017.12

Morton, F.I., 1986. Practical Estimates of Lake Evaporation. J. Clim. Appl. Meteorol. 25, 371–387. https://doi.org/10.1175/1520-0450(1986)025<0371:PEOLE>2.0.CO;2

Okonkwo, C., Demoz, B., Sakai, R., Ichoku, C., Anarado, C., Adegoke, J., Amadou, A., Abdullahi, S.I., 2015. Combined effect of El Niño southern oscillation and Atlantic multidecadal oscillation on Lake Chad level variability. Cogent Geosci. 1, 1117829. https://doi.org/10.1080/23312041.2015.1117829

Okpara, U.T., Stringer, L.C., Dougill, A.J., 2016. Lake drying and livelihood dynamics in Lake Chad: Unravelling the mechanisms, contexts and responses. Ambio 45, 781–795.

https://doi.org/10.1007/s13280-016-0805-6

Policelli, F., Hubbard, A., Jung, H.C., Zaitchik, B., Ichoku, C., 2018a. Lake Chad Total Surface Water Area as Derived from Land Surface Temperature and Radar Remote Sensing Data. Remote Sens. 10, 252. https://doi.org/10.3390/rs10020252

Policelli, F., Hubbard, A., Jung, H.C., Zaitchik, B., Ichoku, C., 2018b. A predictive model for Lake Chad total surface water area using remotely sensed and modeled hydrological and meteorological parameters and multivariate regression analysis, Journal of Hydrology, Volume 568, January 2019, Pages 1071-1080 https://doi.org/10.1016/j.jhydrol.2018.11.037

Riahi, K., Rao, S., Krey, V., Cho, C., Chirkov, V., Fischer, G., Kindermann, G., Nakicenovic, N., Rafaj, P., 2011. RCP 8.5—A scenario of comparatively high greenhouse gas emissions Climatic Change 109, 33. https://doi.org/10.1007/s10584-011-0149-y

Ricko, M., Carton, J.A., Birkett, C.M., Cretaux, J.-F., 2012. Intercomparison and validation of continental water level products derived from satellite radar altimetry. J. Appl. Remote Sens. 6, 061710. https://doi.org/10.1117/1.JRS.6.061710

Rigal, D., 1989 Crue et décrue au lac Tchad: essai de suivi à partir des images NOAA, novembre 1988-avril 1989. *Veille Climate Satellitaire*, *28*, 71–76.

Rodell, M., Houser, P.R., Jambor, U., Gottschalck, J., Mitchell, K., Meng, C.-J., Arsenault, K., Cosgrove, B., Radakovich, J., Bosilovich, M., Entin, J.K., Walker, J.P., Lohmann, D., Toll, D., 2004. The Global Land Data Assimilation System. Bull. Am. Meteorol. Soc. 85,

381–394. https://doi.org/10.1175/BAMS-85-3-381

Sarch, M.-T., Birkett, C., 2000. Fishing and farming at Lake Chad: Responses to lake-level fluctuations. Geogr. J. 166, 156–172.

Sass, G.Z.; Creed, I.F., 2008 Characterizing hydrodynamics on boreal landscapes using archived synthetic aperture radar imagery. *Hydrol. Process.*, *22*, 1687–1699.

Satellite Radar Altimetry: Global Reservoir and Lake Elevation Database [WWW Document], no date URL https://www.pecad.fas.usda.gov/cropexplorer/global_reservoir/ (accessed 10.17.17).

Schneider, Udo; Becker, Andreas; Finger, Peter; Meyer-Christoffer, Anja; Rudolf, Bruno; Ziese, Markus (2015): GPCC Full Data Monthly Product Version 7.0 at 0.5º: Monthly Land-Surface Precipitation from Rain-Gauges built on GTS-based and Historic Data. DOI: 10.5676/DWD GPCC/FD M V7 050

Schuster, M., Roquin, C., Duringer, P., Brunet, M., Caugy, M., Fontugne, M., Taïsso Mackaye, H., Vignaud, P., Ghienne, J.-F., 2005. Holocene Lake Mega-Chad palaeoshorelines from space. Quaternary Science Reviews 24, 1821–1827. https://doi.org/10.1016/j.quascirev.2005.02.001

Senay, G.B., Bohms, S., Singh, R.K., Gowda, P.H., Velpuri, N.M., Alemu, H., Verdin, J.P., 2013 Operational Evapotranspiration Mapping Using Remote Sensing and Weather Datasets: A New Parameterization for the SSEB Approach. JAWRA J. Am. Water Resour. Assoc.

49, 577–591. https://doi.org/10.1111/jawr.12057

Sheffield, J., Goteti, G., Wood, E.F., 2006. Development of a 50-Year High-Resolution Global Dataset of Meteorological Forcings for Land Surface Modeling. J. Clim. 19, 3088–3111. https://doi.org/10.1175/JCLI3790.1

Sylla, M.B.; Giorgi, F.; Coppola, E.; Mariotti, L., 2013. Uncertainties in daily rainfall over Africa: assessment of gridded observation products and evaluation of a regional climate model simulation. *Int. J. Climatol. 33*, 1805–1817.

Taylor, K.E., Stouffer, R.J., Meehl, G.A., 2011. An Overview of CMIP5 and the Experiment Design. Bull. Amer. Meteor. Soc. 93, 485–498. https://doi.org/10.1175/BAMS-D-11-00094.1

UNEP (a) /Earthprint, 2006; Belgium. Administration générale de la coopération au développement. *Africa's Lakes: Atlas of Our Changing Environment*; Available online: http://www.historylab.unina2.it/files/249.pdf (accessed on 18 January 2018).

UNEP (b) United Nations Environment Programme. Available online: http://www7.dict.cc/wp_examples.php?lp_id=1&lang=en&s=United%20Nations%20Environment%20Programme (accessed on 21 July 2017).

Vuuren, D.P. van, Edmonds, J., Kainuma, M., Riahi, K., Thomson, A., Hibbard, K., Hurtt, G.C., Kram, T., Krey, V., Lamarque, J.-F., Masui, T., Meinshausen, M., Nakicenovic, N., Smith, S.J., Rose, S.K., 2011. The representative concentration pathways: an overview. Climatic Change 109, 5. https://doi.org/10.1007/s10584-011-0148-z

Wan, Z.; H, S. MOD11A2 MODIS/Terra Land Surface Temperature/Emissivity 8-Day L3 Global 1km SIN Grid V006 2015. Available online: https://lpdaac.usgs.gov/dataset_discovery/modis/modis_products_table/mod11a2_v006 (accessed on 1 January 2018).

Wan, Z.; H, S. MOD11A1 MODIS/Terra Land Surface Temperature/Emissivity Daily L3 Global 1km SIN Grid V006 2015. Available online: https://lpdaac.usgs.gov/dataset_discovery/modis/modis_products_ table/mod11a1_v006 (accessed on 1 January 2018).

White, L., Brisco, B., Dabboor, M., Schmitt, A., Pratt, A., 2015. A Collection of SAR Methodologies for Monitoring Wetlands. Remote Sensing 7, 7615–7645. https://doi.org/10.3390/rs70607615

Wilusz, D.C.; Zaitchik, B.F.; Anderson, M.C.; Hain, C.R.; Yilmaz, M.T.; Mladenova, I.E. Monthly flooded area classification using low resolution SAR imagery in the Sudd wetland from 2007 to 2011. *Remote Sens. Environ.* **2017**, *194*, 205–218.

Zhu, W., Yan, J., Jia, S., 2017a. Monitoring Recent Fluctuations of the Southern Pool of Lake Chad Using Multiple Remote Sensing Data: Implications for Water Balance Analysis. Remote Sens. 9, 1032. https://doi.org/10.3390/rs9101032

Biography

Frederick “Fritz” Policelli was born in 1964 in Princeton, New Jersey USA.

Frederick did his undergraduate work at Cornell University where he majored in mechanical engineering. Following graduation from Cornell, Frederick moved to Connecticut where he worked for Pratt and Whitney on commercial jet engines, married his wife of twenty-eight years, and worked nights on his master’s degree through Rensselaer Polytechnic Institute at the Hartford Graduate Center.

Frederick went to work for NASA as a propulsion test engineer at the Stennis Space Center in 1991. After a career change to Earth sciences within NASA in 1998, Frederick transferred to the NASA Goddard Space Flight Center (GSFC) in 2003. In 2013, while working at GSFC, Frederick started work on his doctoral degree in Earth and Planetary Sciences at Johns Hopkins University.